Current Research in Environmental & Applied Mycology (Journal of Fungal Biology)
12(1): 285–321 (2022) ISSN 2229-2225
www.creamjournal.org

Article

Doi 10.5943/cream/12/1/18

Pestalotioid species associated with palm species from Southern China

Xiong YR[1,2,5], Manawasinghe IS[1*], Maharachchikumbura SSN[3], Lu L[2,5,6], Dong ZY[1,4], Xiang MM[1] and Xu B[1]

[1]*Innovative Institute for Plant Health, Zhongkai University of Agriculture and Engineering, Guangzhou 510225, China*
[2]*Center of Excellence in Fungal Research, Mae Fah Luang University, Chiang Rai 57100, Thailand*
[3]*School of Life Science and Technology, Centre for Informational Biology, University of Electronic Science and Technology of China, Chengdu 611731, China*
[4]*Key Laboratory of Green Prevention and Control on Fruits and Vegetables in South China, Ministry of Agriculture and Rural Affairs, China*
[5]*School of Science, Mae Fah Luang University, Chiang Rai 57100, Thailand*
[6]*Center for Yunnan Plateau Biological Resources Protection and Utilization, College of Biological Resource and Food Engineering, Qujing Normal University, Qujing, Yunnan 655011, China*

Xiong YR, Manawasinghe IS, Maharachchikumbura SSN, Lu L, Dong ZY, Xiang MM, Xu B 2022 – Pestalotioid species associated with palm species from Sothern China. Current Research in Environmental & Applied Mycology (Journal of Fungal Biology) 12(1), 285–321, Doi 10.5943/cream/12/1/18

Abstract

Palm is the largest monocot group widely distributed in tropical and subtropical regions. The importance of palm species ranges from food sources to landscape. Therefore, the identification and characterization of pathogens associated with these hosts have economic and ecological significance. During surveys in 2020 to 2021, leaf spots on diseased *Sabal mexicana* and rotting tissues of *Areca triandra*, *Arenga pinnata*, *Dypsis leptocheilos*, *Washingtonia robusta* were collected from three cities in southwestern China. Fungal isolates were identified using morphological characterization and phylogenetic analysis based on the internal transcribed spacer (ITS) region of ribosomal DNA, beta-tubulin (*tub2*) gene and part of the translation elongation factor 1-alpha (*tef* 1-α). Six *Neopestalotiopsis* isolates and 22 *Pestalotiopsis* isolates were obtained. These isolates were further confirmed as two novel species described here as *P. guangdongnsis* and *P. sabal*; and three new host records *N. formicidarum*, *P. diploclisae*, *P. kandelicola*; and one unclassified *Neopestalotiopsis* sp. Pathogenicity assays were conducted on potted *Sabal mexicana* leaves for all isolated taxa. The results revealed that all species isolated from this study induced weak lesions on *Sabal mexicana* leaves. Pathogens were reisolated, and Koch's postulates were fulfilled. The results from this study will be an addition to micro-fungi associated with palm trees. Moreover, pathogenicity test results revealed the opportunistic nature of pestalotioid species on *Sabal mexicana*. These results will provide a basic platform to understand the pathogenic mechanisms and lifestyle of pestalotioid species in the future.

Keywords – 2 new species – 3 new host records – *Neopestalotiopsis* – *Pestalotiopsis* – Pathogenicity – *Sporocadaceae*

Introduction

Palm trees (*Arecaceae*) are important and more prominent in the tropics due to their extensive uses as food sources, construction materials, handicrafts, landscaping, and alternative medicine

Submitted 25 August 2022, Accepted 19 October 2022, Published 16 November 2022
Corresponding Author: I.S. Manawasinghe – e-mail – ishara9017@gmail.com

(Mendes et al. 2019). In addition, the beauty and uniqueness of palm plants in tropical landscapes are aesthetically important (Dransfield et al. 2008). *Arecaceae* is a monotypic family in Arecales and contains many important commercial species, such as coconuts, oil palm, and date palm, as well as many ornamental species (Basu et al. 2014). In addition, *Arecaceae* has almost all possible androgynous and/or unisexual flower combinations (Selmaoui et al. 2014). It includes about 2,600 species, divided into climbing plants, shrubs, trees belonging to 181 genera (Baker & Dransfield 2016, Nadot et al. 2016). These species are distributed globally in tropical and subtropical regions, and their abundance also impacts the structure of forests (Bacon & Bailey 2006).

Studies on palm species mainly focus on addressing their commercial uses, such as food's economic and environmental effects (Mendes et al. 2019, Gutiérrez del Pozo et al. 2020, Hassan et al. 2021). In recent years, several pests and diseases afflicting palm trees have been reported increasingly (Haq & Ijaz 2020, Rajesh et al. 2021). Among them fungal diseases occupy a significant place, affecting commercial and landscaping palm species (Dransfield et al. 2008, Rajesh et al. 2021). Fungal diseases associated with palm hosts are mainly; bud rot/ fruit rot caused by *Phytophthora palmivora*, stem bleeding disease caused by *Thielaviopsis paradoxa*, leaf spot/leaf blight caused by *Bipolaris incurvata*, *Helminthosporium* sp., *Pestalotia palmarum*, and basal stem rot caused by *Ganoderma* sp. (Rajesh et al. 2021, Pandian et al. 2021). However, besides the studies of Fröhlich et al. and Hyde et al. (Fröhlich & Hyde 2000, Hyde et al. 2000), little is known about the micro-fungi associated with *Arecaceae* species.

Eriksson and Hawksworth (1986) introduced Amphisphaeriales in the subclass Xylariomycetidae. Based on the phylogenetic analyses, Hyde et al. (2020a) accepted 17 families in this order. *Sporocadaceae* is one of the largest families in Amphisphaeriales. Jaklitsch et al. (2016) re-validated *Sporocadaceae* and included 22 genera, including *Bartaliniaceae*, *Discosiaceae*, *Pestalotiopsidaceae* and *Robillardaceae* are synonymous under *Sporocadaceae*. *Sporocadaceae* is a species-rich family with endophytes, phytopathogens and saprobes on a wide range of hosts (Liu et al. 2019). Hyde et al. (2020a) and Wijayawardene et al. (2020, 2022) revised *Sporocadaceae* into Amphisphaeriales and accepted 35 genera, including *Neopestalotiopsis*, *Pestalotiopsis,* and *Pseudopestalotiopsis*.

Steyaert (1949) proposed *Pestalotia* and *Pestalotiopsis*, but there had been controversy about the correct classification of these genera. The morphological features of *Pestalotiopsis* were not fully accepted until the evidence of electron microscopy (Guba 1960, Steyaert 1963, Griffiths & Swart 1974a, 1974b, Sutton 1980). Nag Raj (1985) redefined the type species of *Pestalotiopsis*. *Neopestalotiopsis* was introduced by Maharachchikumbura et al. (2014) based on previous studies combined with phylogenetic analysis. This genus is characterized by versicolorous median cells in conidia, whereas *Pseudopestalotiopsis* characterized by indistinct conidiophores and *Pestalotiopsis* with generally dark coloured concolourous median cells. There are 336 species listed in *Pestalotiopsis* in Species Fungorum and MycoBank (20/7/2022), yet this genus still has considerable biodiversity that can be exploited (Hyde et al. 2020a). To date, 68 *Neopestalotiopsis* epithets are available in Species Fungorum and MycoBank (20/7/2022). Many novel *Neopestalotiopsis* species were introduced in China and Thailand during the last few years (Norphanphoun et al. 2019, Yang et al. 2021).

Pestalotioid taxa (*Neopestalotiopsis*, *Pestalotiopsis*, *Pseudopestalotiopsis*) are endophytes, pathogens, or saprobes on a wide range of hosts (Maharachchikumbura et al. 2014, Hyde et al. 2016, Reddy et al. 2016, Ran et al. 2017, Freitas et al. 2019, Yang et al. 2021). These species are commonly reported to cause fruit rots, leaf blights, leaf spots, stem rots, gray blights, scabby cankers, and post-harvest rots (Maharachchikumbura et al. 2014, Lu et al. 2015, Guo et al. 2016, Li et al. 2016, Ismail et al. 2017, Amrutha & Vijayaraghavan 2018, Gerardo-Lugo et al. 2020, Silva et al. 2020, Darapanit et al. 2021). *Pestalotiopsis* includes the most significant number of reported pathogens among the three pestalotioid genera. *Pestalotiopsis aeruginea*, *P. espaillatii*, *P. furcata*, *P. palmarum*, *P. versicolor* and *P. virgatula* are well-known for causing leaf blight and fruit rot in a number of plants (Suwannarach et al. 2012, Maharachchikumbura et al. 2013a, Norphanphoun et al. 2019, Darapanit et al. 2021). In contrast, *Neopestalotiopsis* has the fewest pathogenic records, which includes *N. clavispora*, *N. piceana* and *N. samarangensis* (Maharachchikumbura et al. 2013b, Norphanphoun et al. 2019, Darapanit et al. 2021). Among a wide range of hosts, palms are one easy target of infection by these fungi (Selmaoui et al. 2014, Basavand et al. 2020).

Even though pestalotioid species are characterized and identified from several palm plants as pathogens, none of these studies has discussed explicitly whether these fungi act as opportunistic fungal pathogens or otherwise. Moreover, it remains to understand whether these fungi can complete their life cycles within a host as endophytes, pathogens, and saprobes. Given these facts, the objectives of this study were to identify pestalotioid taxa from palm hosts (*Arecaceae*) and explore the pathogenicity of isolated strains from dead tissues and disease leaves. Saprobic samples were collected from five species belongs to *Arecaceae*; *Areca triandra*, *Arenga pinnata*, *Dypsis leptocheilos*, *Washingtonia robusta* and pathogens were isolated from *Sabal mexicana* (*Arecaceae*) living plants. Species were isolated and identified following polyphasic approaches. Pathogenicity essays were conducted on potted *Sabal mexicana*.

Materials & Methods

Samples collection and Isolation

Saprobic and pathogenic samples were collected from major botanical gardens in Guangzhou and Shenzhen in Guangdong Province and Kunming in Yunnan Province, China. These samples, four of which were saprophytic and one pathogenic, included leaf lamina, rotting leaves, and sheaths belonging to five palm species in five genera. The five species and their corresponding genera are *Areca triandra* (*Areca*), *Arenga pinnata* (*Arenga*), *Dypsis leptocheilos* (*Dypsis*), *Sabal mexicana* (*Sabal*), *Washingtonia robusta* (*Washingtonia*). Both saprobic and pathogenic samples were taken into the laboratory using ziplock bags. After the saprobic samples were brought into the laboratory, following Choi & Hyde (1999), single spore isolations were carried out and pure cultures were obtained (Senanayake et al. 2020). When pathogenic samples were collected, relevant photographs were taken, and disease symptoms were recorded (Fig 1). The pathogen isolation was done following the tissue isolation method described by Zhang et al. (2020). Diseased tissues (neighboring the asymptomatic regions) were cut into small pieces (5 × 5 mm) using sterilized scissors. After surface sterilization, 75% ethanol for 30s, washed three times in sterile water and dried on sterilized filter paper, tissues were placed in potato dextrose agar (PDA) plates and incubated at 25ºC for 5 days, and the individual colonies were transferred to new PDA plates. The single-spore method was used to obtain a pure culture (Senanayake et al. 2020). Isolates were transferred to new potato dextrose agar (PDA) plates to obtain pure cultures. All cultures obtained in this study were deposited in the culture collection of Zhongkai University of Agriculture and Engineering (ZHKUCC). Herbarium materials were deposited at Zhongkai University of Agriculture and Engineering (ZHKU).

Morphological characterization

After the saprobic samples were taken into the laboratory, the Cnoptec SZ650 (China) series stereomicroscope was used to observe the macro-morphological characteristics. A Nikon Eclipse 80i and the industrial DigitaL Sight DS-Fi1 (Panasonic, Japan) microscope imaging system was used to take pictures. For pathogenic isolates, pure cultures sporulated on potato dextrose agar (PDA) were used for macro- and micro-morphological characterization. Digital images of micro-morphological structures, including shape, size, and colour were recorded. Conidial length, width, and size of appendages were measured for 40 conidia per isolate, using NISElements BR 3.2, and the mean values were calculated with their standard deviations (SDs). All pure cultures obtained in this study (both pathogenic and saprobic) were grown on PDA at 25ºC under 12 hours of daylight for one week, and the diameter of the cultures were measured after 7 days. Colony colour (top and bottom) was described by referring to the Rayner (1970) colour chart.

DNA extraction, PCR amplification and sequencing

From pure cultures grown on PDA for 5–7 days, approximately 500 mg of fresh fungal mycelium was scraped. The total genomic DNA was extracted using MagPure Plant AS Kit (magnetic bead hair plant DNA kit) following the manufacturer's instructions. Three nuclear gene regions, internal transcribed spacer (ITS), beta-tubulin (*tub2*) and translation elongation factor 1-alpha (*tef* 1-α) were amplified using the primers shown in Table 1. The PCR reaction mixture contained 25 µL of total volume, which consisted of 12.5 µL 2 FastTaq Premix (mixture of FastTaq TM DNA Polymerase, buffer, dNTP Mixture, and stabilizer) (Beijing Qingke Biological Technology Co., Ltd., Beijing, China), 1 µL of each forward and reverse primers, 9.5 µL ddH2O and 1 µL DNA. The polymerase chain reaction was performed in a C1000 TouchTM thermal cycler. The respective reaction conditions for each gene region are given in Table 1. The positive implications were observed after 1 % agarose gel electrophoresis under ultraviolet light using GelDoc XR$^+$ (BIO-RAD, USA). DNA sequencing was carried out by Tianyi (Guangzhou, China) Co., Ltd. All sequence data generated in this study are deposited in NCBI GenBank (Table 2).

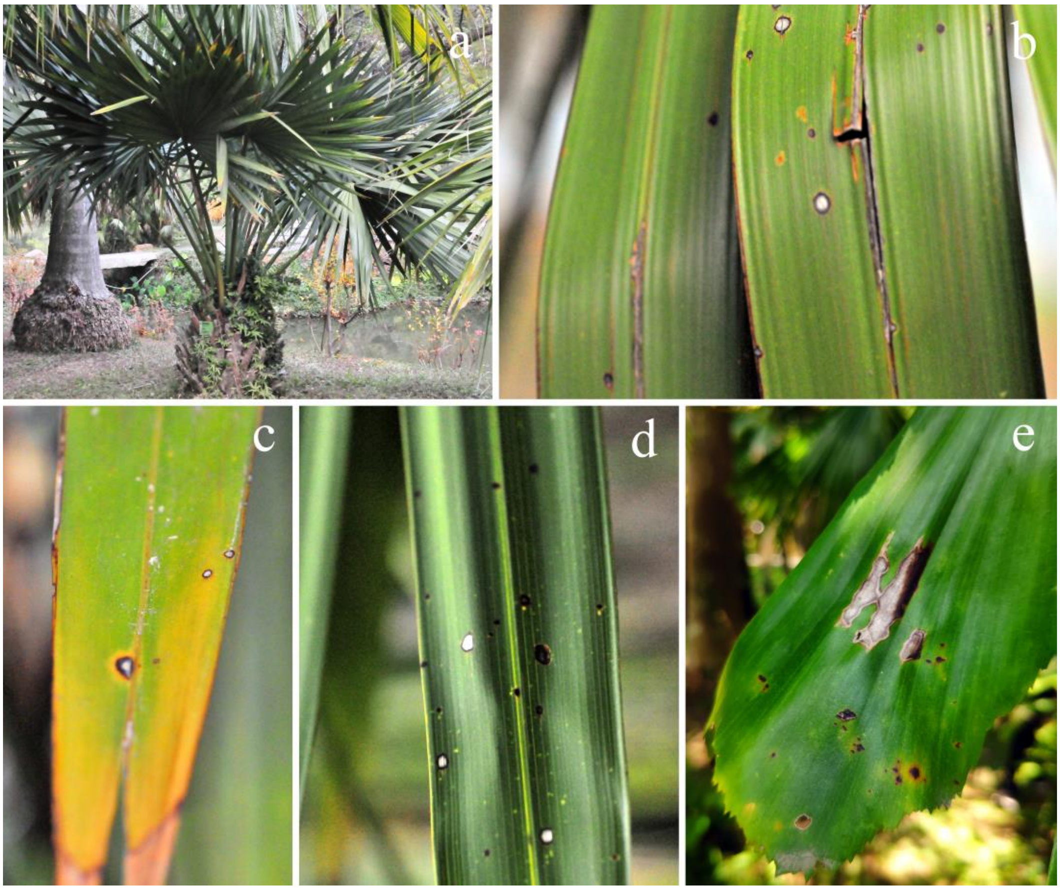

Fig. 1 – Field samples of palm species. a A *Sabal Mexicana*. b-d Leaf spots on *Sabal Mexicana*. e Leaf spots on *Caryota mitis*.

Table 1 Gene regions, respective primer pairs and thermal cycler conditions used in this study.

Gene	Primer Sequence (5'–3')	Amplification	Reference
ITS	ITS5: GGAAGTAAAAGTCGTAACAAGG ITS4: TCCTCCGCTTATTGATATGC	Initial denaturation at 95ºC for 2 mins, followed by 39 cycles consisting of denaturation at 95ºC for 1 min, annealing at 50ºC for 1 min, extension at 72ºC for 1 min, and a final extension at 72ºC for 10 mins	White et al. (1990)

Table 1 Continued.

Gene	Primer Sequence (5'–3')	Amplification	Reference
tub2	T1: AACATGCGTGAGATTGTAAGT Bt2b: CCRGAYTGRCCRAARACRAAGTTGTC	Initial denaturation at 94ºC for 2 min, followed by 30 cycles consisting of denaturation at 94ºC for 50 s, annealing at 55ºC for 1 min, extension at 72ºC for 1 min, and a final extension at 72ºC for 10 mins.	Glass & Donaldson (1995)
tef 1-α	EF1–728F: CATCGAGAAGTTCGAGAAGG EF1–986R: TACTTGAAGGAACCCTTACC	Initial denaturation at 95ºC for 2 mins, followed by 35 cycles consisting of denaturation at 95ºC for 1 min, annealing at 52ºC for 1 min, extension at 72ºC for 1 min, and a final extension at 72 ˚C for 7 mins.	Carbone & Kohn (1999)

Table 2 *Neopestalotiopsis* and *Pestalotiopsis* species and isolates used in the phylogenetic analyses, with GenBank accession numbers.

Species	Strain	ITS	*tub2*	*tef* 1-α	Reference
Neopestalotiopsis acrostichi	MFLUCC 17–1754 T	MK764272	MK764338	MK764316	Norphanphoun et al. (2019)
	MFLUCC 17–1755	MK764273	MK764339	MK764317	Norphanphoun et al. (2019)
N. alpapicalis	MFLUCC 17–2544 T	MK357772	MK463545	MK463547	Kumar et al. (2019)
	MFLUCC 17–2545	MK357773	MK463546	MK463548	Kumar et al. (2019)
N. aotearoa	CBS 367.54 T	KM199369	KM199454	KM199526	Maharachchikumbura et al. (2014)
N. asiatica	MFLUCC 12–0286 T	JX398983	JX399018	JX399049	Maharachchikumbura et al. (2014)
N. australis	CBS 114159 T	KM199348	KM199432	KM199537	Maharachchikumbura et al. (2014)
N. brachiata	MFLUCC 17–555 T	MK764274	MK764340	MK764318	Norphanphoun et al. (2019)
N. brasiliensis	COAD 2166 T	MG686469	MG692400	MG692402	Bezerra et al. (2018)
N. cavernicola	KUMCC 20–0269 T	MW545802	MW557596	MW550735	Liu et al. (2021)
	KUMCC 20–0332	MW581238	MW590328	MW590327	Liu et al. (2021)
N. chiangmaiensis	MFLUCC 18–0113 T	N/A	MH412725	MH388404	Tibpromma et al. (2018)
N. chrysea	MFLUCC 12–0261 T	JX398985	JX399020	JX399051	Maharachchikumbura et al. (2012)
	MFLUCC 12–0262	JX398986	JX399021	JX399052	Maharachchikumbura et al. (2012)
N. clavispora	MFLUCC 12–0280	JX398978	JX399013	JX399044	Maharachchikumbura et al. (2012)
	MFLUCC 12–0281 T	JX398979	JX399014	JX399045	Maharachchikumbura et al. (2012)
N. cocoës	MFLUCC 15–0152 T	KX789687	N/A	KX789689	Hyde et al. (2016)
N. coffeae-arabicae	HGUP4015	KF412647	KF412641	KF412644	Song et al. (2013)
	HGUP4019 T	KF412649	KF412643	KF412646	Song et al. (2013)
N. cubana	CBS 600.96 T	KM199347	KM199438	KM199521	Maharachchikumbura et al. (2014)
N. dendrobii	MFLUCC 14–0099	MK993570	MK975834	MK975828	Ma et al. (2019)
	MFLUCC 14–0106 T	MK993571	MK975835	MK975829	Ma et al. (2019)
N. drenthii	BRIP 72263a T	MZ303786	MZ312679	MZ344171	Prasannath et al. (2021)
	BRIP 72264a	MZ303787	MZ312680	MZ344172	Prasannath et al. (2021)
N. egyptiaca	CBS H 22294 T	KP943747	KP943746	KP943748	Crous et al. (2015)

Table 2 Continued.

Species	Strain	ITS	*tub2*	*tef* 1-α	Reference
N. ellipsospora	MFLUCC 12–0283 T	JX398980	JX399016	JX399047	Maharachchikumbura et al. (2012)
N. eucalypticola	CBS 264.37 T	KM199376	KM199431	KM199551	Maharachchikumbura et al. (2014)
N. foedans	CGMCC 3.9123 T	JX398987	JX399022	JX399053	Maharachchikumbura et al. (2012)
	CGMCC 3.9178	JX398989	JX399024	JX399055	Maharachchikumbura et al. (2012)
N. formicidarum	CBS 362.72 T	KM199358	KM199455	KM199517	Maharachchikumbura et al. (2014)
	CBS 115.83	KM199344	KM199444	KM199519	Maharachchikumbura et al. (2014)
	PSU-T-L01	LC521858	LC521879	LC521873	Pornsuriya et al. (2020)
	INPA 2917	MN267738	MN313573	MN267741	Gualberto et al. (2021)
	ZHKUCC 22–0013	ON158793	ON221567	ON221539	This study
	ZHKUCC 22–0014	ON158794	ON221568	ON221540	This study
	ZHKUCC 22–0015	ON158795	ON221569	ON221541	This study
N. hadrolaeliae	VIC 47180 T	MK454709	MK465120	MK465122	Freitas et al. (2019)
	VIC 47181	MK454710	MK465121	MK465123	Freitas et al. (2019)
N. honoluluana	CBS 111535	KM199363	KM199461	KM199546	Maharachchikumbura et al. (2014)
	CBS 114495 T	KM199364	KM199457	KM199548	Maharachchikumbura et al. (2014)
N. hydeana	MFLUCC 20–0132 T	MW266069	MW251119	MW251129	Huanaluek et al. (2021)
N. iranensis	CBS 137767	KM074045	KM074056	KM074053	Ayoubi & Soleimani (2016)
	CBS 137768 T	KM074048	KM074057	KM074051	Ayoubi & Soleimani (2016)
N. javaensis	CBS 257.31 T	KM199357	KM199437	KM199543	Maharachchikumbura et al. (2014)
N. keteleeria	MFLUCC 13–0915	KJ023087	KJ023088	KJ023089	Song et al. (2014a)
N. macadamiae	BRIP 63737c T	KX186604	KX186654	KX186627	Akinsanmi et al. (2017)
	BRIP 63742a	KX186599	KX186657	KX186629	Akinsanmi et al. (2017)
N. maddoxii	BRIP 72266a T	MZ303782	MZ312675	MZ344167	Prasannath et al. (2021)
N. magna	MFLUCC 12–652 T	KF582795	KF582793	KF582791	Maharachchikumbura et al. (2013c)
N. mesopotamica	CBS 299.74	KM199361	KM199435	KM199541	Maharachchikumbura et al. (2014)
	CBS 336.86 T	KM199362	KM199441	KM199555	Maharachchikumbura et al. (2014)
N. musae	MFLUCC 15–0776 T	KX789683	KX789686	KX789685	Hyde et al. (2016)
N. natalensis	CBS 138.41 T	KM199377	KM199466	KM199552	Maharachchikumbura et al. (2014)
N. nebuloides	BRIP 66617 T	MK966338	MK977632	MK977633	Crous et al. (2020)
N. olumideae	BRIP 72273a T	MZ303790	MZ312683	MZ344175	Prasannath et al. (2021)
N. pernambucana	URM 7148	KJ792466	N/A	KU306739	Silvério et al. (2016)
	RV02	KJ792467	N/A	KU306740	Silvério et al. (2016)
N. petila	MFLUCC 17–1737 T	MK764275	MK764341	MK764319	Norphanphoun et al. (2019)
	MFLUCC 17–1738	MK764276	MK764342	MK764320	Norphanphoun et al. (2019)
N. phangngaensis	MFLUCC 18–0119 T	MH388354	MH412721	MH388390	Tibpromma et al. (2018)
	MFLU 19–2741	MW114333	MW148259	MW192200	N/A
N. piceana	CBS 254.32	KM199372	KM199452	KM199529	Maharachchikumbura et al. (2014)

Table 2 Continued.

Species	Strain	ITS	*tub2*	*tef* 1-α	Reference
	CBS 394.48 T	KM199368	KM199453	KM199527	Maharachchikumbura et al. (2014)
N. protearum	CBS 114178 T	JN712498	KM199463	LT853201	Maharachchikumbura et al. (2014)
N. rhapidis	GUCC 21501	MW931620	MW980441	MW980442	Yang et al. (2021)
N. rhizophorae	MFLUCC 17–1550 T	MK764277	MK764343	MK764321	Norphanphoun et al. (2019)
	MFLUCC 17–1551	MK764278	MK764344	MK764322	Norphanphoun et al. (2019)
N. rhododendri	GUCC 21504	MW979577	MW980443	MW980444	Yang et al. (2021)
	GUCC 21505	MW979576	MW980445	MW980446	Yang et al. (2021)
N. rosae	CBS 101057 T	KM199359	KM199429	KM199523	Maharachchikumbura et al. (2014)
	CBS 124745	KM199360	KM199430	KM199524	Maharachchikumbura et al. (2014)
N. rosicola	CFCC 51992 T	KY885239	KY885245	KY885243	Jiang et al. (2018)
	CFCC 51993	KY885240	KY885246	KY885244	Jiang et al. (2018)
N. samarangensis	CBS 115451	KM199365	KM199447	KM199556	Maharachchikumbura et al. (2013b)
N. saprophytica	MFLUCC 12–0282 T	JX398982	JX399017	JX399048	Maharachchikumbura et al. (2012)
N. sichuanensis	CFCC 54338 T = SM15–1	MW166231	MW218524	MW199750	Jiang et al. (2021)
	SM15–1C	MW166232	MW218525	MW199751	Jiang et al. (2021)
N. sonneratae	MFLUCC 17–1744 T	MK764279	MK764345	MK764323	(Norphanphoun et al. 2019)
	MFLUCC 17–1745	MK764280	MK764346	MK764324	Norphanphoun et al. (2019)
Neopestalotiopsis sp.	ZHKUCC 22–0019	ON158796	ON221514	ON221542	This study
	ZHKUCC 22–0020	ON158797	ON221515	ON221543	This study
	ZHKUCC 22–0021	ON158798	ON221516	ON221544	This study
N. steyaertii	IMI 192475 T	KF582796	KF582794	KF582792	Jiang et al. (2021)
N. surinamensis	CBS 450.74 T	KM199351	KM199465	KM199518	Maharachchikumbura et al. (2014)
N. thailandica	MFLUCC 17–1730 T	MK764281	MK764347	MK764325	Norphanphoun et al. (2019)
	MFLUCC 17–1731	MK764282	MK764348	MK764326	Norphanphoun et al. (2019)
N. umbrinospora	MFLUCC 12–0285 T	JX398984	JX399019	JX399050	Maharachchikumbura et al. (2012)
N. vheenae	BRIP 72293a T	MZ303792	MZ312685	MZ344177	Prasannath et al. (2021)
N. vitis	MFLUCC 15–1265 T	KU140694	KU140685	KU140676	Jayawardena et al. (2016)
	MFLUCC 15–1270	KU140699	KU140690	KU140681	Jayawardena et al. (2016)
N. zakeelii	BRIP 72282a T	MZ303789	MZ312682	MZ344174	Prasannath et al. (2021)
N. zimbabwana	CBS 111495 T	JX556231	KM199456	KM199545	Maharachchikumbura et al. (2014)
Pestalotiopsis. adusta	ICMP 6088 T	AF409957	JX399037	JX399070	Maharachchikumbura et al. (2012)
	MFLUCC 10–0146	JX399007	JX399038	JX399071	Maharachchikumbura et al. (2012)
P. aggestorum	LC6301 T	KX895015	KX895348	KX895234	Liu et al. (2017)
	LC8186	KY464140	KY464160	KY464150	Liu et al. (2017)
P. anacardiacearum	IFRDCC 2397 T	KC247154	KC247155	KC247156	Maharachchikumbura et al. (2013d)

Table 2 Continued.

Species	Strain	ITS	*tub2*	*tef* 1-α	Reference
	HN37–4	N/A	MK360932	MK512485	Shu et al. (2020)
	YB41–2	N/A	MK360933	MK512486	Shu et al. (2020)
	FY10–12	N/A	MK360931	MK512484	Shu et al. (2020)
P. arceuthobii	CBS 434.65 [T]	NR147561	KM199427	KM199516	Maharachchikumbura et al. (2014)
P. arengae	CBS 331.92 [T]	NR147560	KM199426	KM199515	Maharachchikumbura et al. (2014)
P. australasiae	CBS 114126 [T]	NR147546	KM199409	KM199499	Maharachchikumbura et al. (2014)
	CBS 114141	KM199298	KM199410	KM199501	Maharachchikumbura et al. (2014)
P. australis	CBS 111503	KM199331	KM199382	KM199557	Maharachchikumbura et al. (2014)
	CBS 114193	KM199332	KM199383	KM199475	Maharachchikumbura et al. (2014)
P. biciliata	CBS 124463 [T]	KM199308	KM199399	KM199505	Maharachchikumbura et al. (2014)
	CBS 236.38	KM199309	KM199401	KM199506	Maharachchikumbura et al. (2014)
	CBS 790.68	KM199305	KM199400	KM199507	Maharachchikumbura et al. (2014)
P. brachiata	LC2988 [T]	KX894933	KX895265	KX895150	Liu et al. (2017)
	LC8188	KY464142	KY464162	KY464152	Liu et al. (2017)
P. brassicae	CBS 170.26 [T]	KM199379	N/A	KM199558	Maharachchikumbura et al. (2014)
P. camelliae	CBS 443.62	KM199336	KM199424	KM199512	Maharachchikumbura et al. (2014)
	MFLUCC 12–0277 [T]	NR120188	JX399041	JX399074	Zhang et al. (2012a)
P. chamaeropis	CBS 113607	KM199325	KM199390	KM199472	Maharachchikumbura et al. (2014)
	CBS 186.71 [T]	KM199326	KM199391	KM199473	Maharachchikumbura et al. (2014)
P. clavata	MFLUCC 12–0268 [T]	JX398990	JX399025	JX399056	Maharachchikumbura et al. (2012)
P. colombiensis	CBS 118553 [T]	NR147551	KM199421	KM199488	Maharachchikumbura et al. (2014)
P. digitalis	ICMP 5434 [T]	KP781879	KP781883	N/A	Liu et al. (2015)
P. diploclisiae	CBS 115585	KM199315	KM199417	KM199483	Maharachchikumbura et al. (2014)
	CBS 115587 [T]	KM199320	KM199419	KM199486	Maharachchikumbura et al. (2014)
	CBS 115449	KM199314	KM199416	KM199485	Maharachchikumbura et al. (2014)
	ZHKUCC 22–0010	ON180759	ON221545	ON221517	This study
	ZHKUCC 22–0011	ON180760	ON221546	ON221518	This study
	ZHKUCC 22–0012	ON180761	ON221547	ON221519	This study
	ZHKUCC 22–0024	ON180772	ON221558	ON221530	This study
	ZHKUCC 22–0025	ON180776	ON221562	ON221534	This study
	ZHKUCC 22–0026	ON180780	ON221566	ON221538	This study
P. disseminata	CBS 118552	MH553986	MH554652	MH554410	Liu et al. (2019)
	CBS 143904	MH554152	MH554825	MH554587	Liu et al. (2019)
	CPC 29351	MH554166	MH554839	MH554601	Liu et al. (2019)
P. distincta	LC3232	KX894961	KX895293	KX895178	Liu et al. (2017)
	LC8184	KY464138	KY464158	KY464148	Liu et al. (2017)
P. diversiseta	MFLUCC 12–0287 [T]	JX399009	JX399040	JX399073	Maharachchikumbura et al. (2012)

Table 2 Continued.

Species	Strain	ITS	*tub2*	*tef* 1-α	Reference
P. doitungensis	MFLUCC 14–0090	MK993573	MK975836	MK975831	Ma et al. (2019)
P. dracaenae	HGUP4037 T	MT596515	MT598645	MT598644	Ariyawansa et al. (2015)
P. dracaenicola	MFLUCC 18–0913 T	MN962731	N/A	N/A	Chaiwan et al. (2020)
	MFLUCC 18–0914	MN962734	N/A	N/A	Chaiwan et al. (2020)
P. dracontomelon	MFLUCC 10–0149	KP781877	N/A	KP781880	Liu et al. (2015)
P. ericacearum	IFRDCC 2439 T	KC537807	KC537821	KC537814	Zhang et al. (2013)
P. etonensis	BRIP 66615 T	MK966339	MK977634	MK977635	Crous et al. (2020)
P. formosana	NTUCC 17–009 T	MH809381	MH809385	MH809389	Ariyawansa & Hyde (2018)
	NTUCC 17–010	MH809382	MH809386	MH809390	Ariyawansa & Hyde (2018)
P. furcata	LC6303	KX895016	KX895349	KX895235	Liu et al. (2017)
	MFLUCC 12–0054 T	JQ683724	JQ683708	JQ683740	Maharachchikumbura et al. (2013a)
P. gaultheri	IFRD 411–014 T	KC537805	KC537819	KC537812	Maharachchikumbura et al. (2014)
P. gibbosa	NOF 3175 T	LC311589	LC311590	LC311591	Watanabe et al. (2018)
P. grevilleae	CBS 114127 T	KM199300	KM199407	KM199504	Maharachchikumbura et al. (2014)
P. guangdongensis	ZHKUCC 22–0016 T	ON180762	ON221548	ON221520	This study
	ZHKUCC 22–0017	ON180763	ON221549	ON221521	This study
	ZHKUCC 22–0018	ON180764	ON221550	ON221522	This study
P. hawaiiensis	CBS 114491 T	NR147559	KM199428	KM199514	Maharachchikumbura et al. (2014)
P. hispanica	CBS 115391	MH553981	MH554640	MH554399	Liu et al. (2019)
P. hollandica	CBS 265.33 T	NR147555	KM199388	KM199481	Maharachchikumbura et al. (2014)
P. humus	CBS 336.97 T	KM199317	KM199420	KM199484	Maharachchikumbura et al. (2014)
P. inflexa	MFLUCC 12–0270 T	JX399008	JX399039	JX399072	Maharachchikumbura et al. (2012)
P. intermedia	MFLUCC 12–0259 T	JX398993	JX399028	JX399059	Maharachchikumbura et al. (2012)
P. italiana	MFLUCC 12–0657 T	KP781878	KP781882	KP781881	Liu et al. (2015)
P. jesteri	CBS 109350 T	KM199380	KM199468	KM199554	Maharachchikumbura et al. (2014)
P. jiangxiensis	LC4399 T	KX895009	KX895341	KX895227	Liu et al. (2017)
P. jinchanghensis	LC6636	KX895028	KX895361	KX895247	Liu et al. (2017)
	LC8190 T	KY464144	KY464164	KY464154	Liu et al. (2017)
P. kaki	KNU-PT-1804 T	LC552953	LC552954	LC553555	Das et al. (2020)
P. kandelicola	NCYUCC 19–0355 T	MT560722	MT563099	MT563101	Hyde et al. (2020b)
	NCYUCC 19–0354	MT560723	MT563100	MT563102	Hyde et al. (2020b)
	ZHKUCC 22–0022	ON180771	ON221557	ON221529	This study
	ZHKUCC 22–0023	ON180779	ON221565	ON221537	This study
P. kenyana	CBS 442.67 T	KM199302	KM199395	KM199502	Maharachchikumbura et al. (2014)
P. knightiae	CBS 114138	KM199310	KM199408	KM199497	Maharachchikumbura et al. (2014)
	CBS 111963	KM199311	KM199406	KM199495	Maharachchikumbura et al. (2014)
P. krabiensis	MFLUCC 16–0260	MH388360	MH412722	MH388395	Tibpromma et al. (2018)
P. leucadendri	CBS 121417	MH553987	MH554654	MH554412	Liu et al. (2019)
P. licualacola	HGUP 4057 T	KC492509	KC481683	KC481684	Geng et al. (2013)
P. linearis	MFLUCC 12–0271	JX398994	JX399027	JX399060	Maharachchikumbura et al. (2012)
P. lushanensis	LC4344 T	KX895005	KX895337	KX895223	Liu et al. (2017)

Table 2 Continued.

Species	Strain	ITS	*tub2*	*tef* 1-α	Reference
	LC8182	KY464136	KY464156	KY464146	Liu et al. (2017)
P. macadamiae	BRIP 63738b T	KX186588	KX186680	KX186620	Akinsanmi et al. (2017)
P. malayana	CBS 102220 T	NR147550	KM199411	KM199482	Maharachchikumbura et al. (2014)
P. monochaeta	CBS 144.97 T	KM199327	KM199386	KM199479	Maharachchikumbura et al. (2014)
	CBS 440.83	KM199329	KM199387	KM199480	Maharachchikumbura et al. (2014)
P. montellica	MFLUCC 12–0279 T	JX399012	JX399043	JX399076	Maharachchikumbura et al. (2012)
P. neglecta	TAP1100	AB482220	LC311599	LC311600	Norphanphoun et al. (2019)
P. neolitseae	NTUCC 17–011 T	MH809383	MH809387	MH809391	Ariyawansa & Hyde (2018)
	NTUCC17012	MH809384	MH809388	MH809392	Ariyawansa & Hyde 2018)
	KUMCC 19–0243	MN625276	MN626730	MN626741	Harishch&ra et al. (2020)
P. novae-hollandiae	CBS 130973 T	NR147557	KM199425	KM199511	Maharachchikumbura et al. (2014)
P. oryzae	CBS 111522 T	KM199294	KM199394	KM199493	Maharachchikumbura et al. (2014)
	CBS 353.69	KM199299	KM199398	KM199496	Maharachchikumbura et al. (2014)
P. pallidotheae	MAFF 240993 T	NR111022	LC311584	LC311585	Watanabe et al. (2010)
P. pandanicola	MFLUCC 16–0255	MH388361	MH412723	MH388396	Tibpromma et al. (2018)
P. papuana	CBS 331.96 T	KM199321	KM199413	KM199491	Maharachchikumbura et al. (2014)
	CBS 887.96	KM199318	KM199415	KM199492	Maharachchikumbura et al. (2014)
	MFLU 19–2764	N/A	MW296942	MW192204	N/A
P. parva	CBS 265.37 T	KM199312	KM199404	KM199508	Maharachchikumbura et al. (2014)
	CBS 278.35	MH855675	KM199405	KM199509	Maharachchikumbura et al. (2014)
P. photinicola	GZCC 16–0028 T	KY092404	KY047663	KY047662	Chen et al. (2017)
P. pini	CBS 146841 T	MT374681	MT374706	MT374694	Silva et al. (2020)
	CBS 146840	MT374680	MT374705	MT374693	Silva et al. (2020)
	CBS 146842	MT374682	MT374707	MT374695	Silva et al. (2020)
	MEAN 1167	MT374689	MT374714	MT374701	Silva et al. (2020)
P. pinicola	KUMCC 19–0203	MN412637	MN417508	MN417510	Tibpromma et al. (2019)
	KUMCC 19–0183	MN412636	MN417507	MN417509	Tibpromma et al. (2019)
P. portugalica	CBS 393.48	KM199335	KM199422	KM199510	Maharachchikumbura et al. (2014)
	LC2929	KX894921	KX895253	KX895138	Liu et al. (2017)
P. rhizophorae	MFLUCC 17–0416 T	MK764283	MK764349	MK764327	Norphanphoun et al. (2019)
	MFLUCC 17–0417	MK764284	MK764350	MK764328	Norphanphoun et al. (2019)
P. rhododendri	IFRDCC 2399	KC537804	KC537818	KC537811	Zhang et al. (2013)
P. rhodomyrtus	LC3413 T	KX894981	KX895313	KX895198	Liu et al. (2017)
	LC4458	KX895010	KX895342	KX895228	Liu et al. (2017)
P. rosea	MFLUCC 12–0258 T	JX399005	JX399036	JX399069	Maharachchikumbura et al. (2012)
P. Sabal	ZHKUCC 22–0027	ON180765	ON221551	ON221523	This study
	ZHKUCC 22–0028	ON180766	ON221552	ON221524	This study

Table 2 Continued.

Species	Strain	ITS	*tub2*	*tef* 1-α	Reference
	ZHKUCC 22–0029	ON180767	ON221553	ON221525	This study
	ZHKUCC 22–0030	ON180768	ON221554	ON221526	This study
	ZHKUCC 22–0031	ON180769	ON221555	ON221527	This study
	ZHKUCC 22–0032	ON180770	ON221556	ON221528	This study
	ZHKUCC 22–0033	ON180773	ON221559	ON221531	This study
	ZHKUCC 22–0034	ON180774	ON221560	ON221532	This study
	ZHKUCC 22–0035 [T]	ON180775	ON221561	ON221533	This study
	ZHKUCC 22–0036	ON180777	ON221563	ON221535	This study
	ZHKUCC 22–0037	ON180778	ON221564	ON221536	This study
P. scoparia	CBS 176.25 [T]	KM199330	KM199393	KM199478	Maharachchikumbura et al. (2014)
P. sequoiae	MFLUCC 13–0399	KX572339	N/A	N/A	Hyde et al. (2016)
P. shandongensis	KUMCC 19–0241	MN625275	MN626729	MN626740	Harishch&ra et al. (2020)
P. shorea	MFLUCC 12–0314 [T]	KJ503811	KJ503814	KJ503817	Song et al. (2014b)
P. spathulata	CBS 356.86	NR147558	KM199423	KM199513	Maharachchikumbura et al. (2014)
P. spathuliappendiculata	CBS 144035	MH554172	MH554845	MH554607	Liu et al. (2019)
P. telopeae	CBS 113606	KM199295	KM199402	KM199498	Maharachchikumbura et al. (2014)
	CBS 114137 [T]	KM199301	KM199469	KM199559	Maharachchikumbura et al. (2014)
	CBS 114161	KM199296	KM199403	KM199500	Maharachchikumbura et al. (2014)
P. terricola	CBS 141.69 [T]	MH554004	MH554680	MH554438	Liu et al. (2019)
P. thailandica	MFLUCC 17–1616 [T]	MK764285	MK764351	MK764329	Norphanphoun et al. 2019)
	MFLUCC 17–1617	MK764286	MK764352	MK764330	Norphanphoun et al. (2019)
P. trachicarpicola	IFRDCC 2440 = OP068 [T]	JQ845947	JQ845945	JQ845946	Zhang et al. (2012b)
P. unicolor	MFLUCC 12–0275 [T]	JX398998	JX399029	JX399063	Maharachchikumbura et al. (2012)
	MFLUCC 12–0276	JX398999	JX399030	JX399063	Maharachchikumbura et al. (2012)
P. verruculosa	MFLUCC 12–0274	JX398996	N/A	JX399061	Maharachchikumbura et al. (2012)
P. yanglingensis	LC3067	KX894949	KX895281	KX895166	Liu et al. (2017)
	LC4553 [T]	KX895012	KX895345	KX895231	Liu et al. (2017)
Pseudopestalotiopsis cocos	CBS 272.29 [T]	KM199378	KM199467	KM199553	Maharachchikumbura et al. (2014)

Notes: BRIP: Queensland Plant Pathology Herbarium, Brisbane, Australia; CBS: Culture Collection of the Westerdijk Fungal Biodiversity Institute, Utrecht, The Netherlands; CFCC: China Forestry Culture Collection Centre, Beijing, China; CGMCC: China General Microbiological Culture Collection Centre, Institute of Microbiology, Chinese Academy of Sciences, Beijing, China; COAD: Coleção Octávio Almeida Drummond, Universidade Federal de Viçosa, Brazil; CPC: Culture collection of Pedro Crous, housed at the Westerdijk Institute; GUCC: Department of Plant Pathology Culture Collection, Agriculture College, Guizhou University, China; GZCC: Guizhou Academy of Agricultural Sciences Culture Collection, Guizhou, China; HGUP: Plant Pathology Herbarium of Guizhou University, Guizhou, China; ICMP: International Collection of Micro-organisms from Plants, Landcare Research, Private Bag 92170, Auckland, New Zealand; IFRD: International Fungal Research and Development; IFRDCC: International Fungal Research and Development Culture Collection; IMI: Culture Collection of CABI Europe UK Centre, Egham, UK; INPA: National Institute of Amazon Research; KNU: Kyungpook National University, Daegu, Korea; KUMCC: Kunming Institute of Botany Culture Collection, Yunnan, China; LC: working collection of Lei Cai, housed at the Institute of Microbiology, Chinese Academy of Sciences, Beijing, China; MAFF: Ministry of Agriculture, Forestry and Fisheries, Tsukuba, Ibaraki, Japan; MEAN: Instituto Nacional de Investigação Agrária e Veterinária I. P.; MFLU: Mae Fah Luang University, Chiang Rai, Thailand; MFLUCC: Mae Fah Luang University Culture Collection, Chiang Rai, Thailand; NCYUCC: National Chiayi University Culture Collection, Chiayi, Taiwan; NOF: The Fungus Culture Collection of the Northern Forestry Centre, Alberta, Canada; NTUCC: the Department of Plant Pathology and Microbiology, National Taiwan University Culture Collection; PSU: Culture Collection of the Pest Management Department, Faculty of Natural Resources, Prince of Songkla University, Thailand; URM: Culture Collection of the Universidade Federal de Pernambuco, Brazil; VIC: Herbarium of the Universidade Federal de Viçosa; ZHKUCC: Zhongkai University of Agriculture and Engineering Culture Collection. Ex-type strains are labelled with T. N/A: Not available. ITS: the internal transcribed spacer, *tub2*: beta-tubulin, *tef* 1-α: translation elongation factor 1-alpha.

Phylogenetic analyses

Sequencing quality was assured by checking sequence chromatograms using Geneious Prime v. 2021.0.3 (Biomatters Ltd., San Diego, CA, USA). The combined sequences were generated using forward and reverse primers by Geneious Prime v. 2021.0.3. The BLASTn tool (Basic Local Alignment Search Tool; https://blast.ncbi.nlm.nih.gov/Blast.cgi) in National Center for Biotechnology Information (NCBI) was used to confirm the genus level of isolated taxa in this study. The reference sequences for phylogenetic analyses were downloaded from GenBank following De silva et al. (2021), Prasannath et al. (2021), and Yang et al. (2021) (Table 2). Using MAFFT v. 7 (https://mafft.cbrc.jp/alignment/server/), the sequences obtained in this study were aligned together with the downloaded sequences. BioEdit 7.0.9.0 was used to manually improve, when necessary. The Alignment Transformation Environment online (https://sing.ei.uvigo.es/ALTER/) was used to convert files to develop phylogenetic trees. Phylogenetic analyses were done using maximum likelihood (ML) inferred in RAxML v. 8.2.12 (Stamatakis 2014), maximum parsimony (MP) implied on PAUP v. 4.0b10 (Swofford 2002), and Bayesian analysis on MrBayes v. 3.1.2 (Huelsenbeck & Ronquist 2001).

Maximum parsimony analysis was performed in PAUP (phylogenetic analysis using parsimony) v.4.0b10 (Swofford 2002) using the heuristic search option with tree bisection-reconnection (TBR) branch swapping and 1000 random sequence additions. Ambiguous regions in the alignment were excluded, and the gaps were treated as missing data. The tree stability was evaluated by 1000 bootstrap replications. Branches of zero lengths were collapsed and all multiple parsimonious trees were saved. Descriptive statistics including tree length (TL), consistency index (CI), retention index (RI), relative consistency index (RC), and homoplasy index (HI) were calculated.

The best model of evolution was determined by MrModeltest v. 2.2 for each gene. Maximum likelihood analyses were accomplished using RAxML-HPC2 on XSEDE v. 8.2.8 (Stamatakis et al. 2008, Stamatakis 2014) in the CIPRES Science Gateway platform (Miller et al. 2010) using the GTR+I+G model of evolution with 1000 non-parametric bootstrapping iterations. MrBayes v.3.0b4 was used for the Bayesian analyses (Huelsenbeck & Ronquist 2001). The Markov Chain Monte Carlo sampling (BMCMC) analysis was conducted with four simultaneous Markov chains. They were run for 1,000,000 generations; sampling the trees at every 100th generation. From the 10,000 trees obtained, the first 2,000 representing the burn-in phase were discarded. The remaining 8,000 trees were used for calculating posterior probabilities in the majority rule consensus tree. Phylogenetic trees were visualized in FigTree v. 1.4.2. Taxonomic novelties were submitted to the Faces of Fungi database (Jayasiri et al. 2015) and Index Fungorum (http://www.indexfungorum.org). Tree alignments are deposited in the TreeBase (https://treebase.org/treebase-web/home.html) under the following IDs: 29488 and 29489.

Pairwise homoplasy index (PHI)

The pairwise homoplasy index (PHI index) was used to confirm newly identified taxa to determine species boundaries (Quaedvlieg et al. 2014). The PHI test was performed using SplitsTree4 v. 4.17.1 (Huson & Bryant 2006) to determine the recombination level within phylogenetically closely related species. The concatenated three-locus dataset (ITS + *tub2* + *tef* 1-α) was used for the analyses. PHI test results (Fw) >0.05 indicated no significant recombination within the dataset. The relationships between closely related taxa were visualized in split graphs via Log-Det transformation and split decomposition options.

Pathogenicity tests

Pathogenicity was tested by mycelial PDA plugs and spore suspensions on potted *Sabal mexicana* leaves. Six pestalotioid species were used to inoculate plants. Both wounded and non-wounded methods were practiced. Foliar surface was first rinsed with sterile water, then the surface sterilized with 75% ethanol for 30 s, rinsed with sterile water three times, and air-dried. For the mycelial plug method, 5 mm diameter hyphal plugs from actively growing seven days old cultures were taken. Using a sterile needle, wounds were created and the mycelial plugs were kept intact and simultaneously. Another plug was placed on the non-wounded surface. Sterilized PDA plugs (5 mm) were used as a control. To inoculate healthy *Sabal mexicana* leaflets 1 × 10^5 spores/mL spore suspension was prepared from each isolate. Once the leaflet was punctured with a sterile needle, and each point was inoculated with 20 µl from spore suspension. Sterile water was used as the control. All the treatments were replicated three times. The inoculated plants were kept in a greenhouse at 70–80% RH and 25ºC. Lesion lengths were recorded starting from ten days after inoculation (dpi).

Results

Phylogenetic analyses

In the present study, 28 pestalotioid isolates were obtained. Following the BLASTn analysis, six isolates were identified as *Neopestalotiopsis* and 22 as *Pestalotiopsis*. Species delineations were based on Chethana et al. (2021), Jayawardena et al. (2021), Maharachchikumbura et al. (2021) and Manawasinghe et al. (2021).

Phylogenetic Analyses of *Neopestalotiopsis*

The concatenated sequence data matrix of the phylogenetic tree comprised 2268 base pairs (bp) (548 for ITS, 952 for *tub2*, and 768 for *tef* 1-α). Similar tree topologies were obtained by ML, MP, and Bayesian methods, and the best-scoring ML tree is shown in Fig. 2. The best scoring ML tree had an optimization likelihood value of -9360.768135. The matrix had 700 distinct alignment patterns with a 26.11% proportion of gaps and completely undetermined characters. Estimated base frequencies were as follows; A = 0.234558, C = 0.275886, G = 0.213950, T = 0.275606; substitution rates: AC = 1.006903, AG = 2.960226, AT = 1.171557, CG = 0.776122, CT = 3.662137, GT = 1.000000; gamma distribution shape parameter α = 0.893849. Incomplete portions at the ends of the sequences were excluded from the analysis. Maximum parsimony analysis yielded a best-scoring tree of which 1439 bp were constant, 450 bp parsimony uninformative, and 308 bp parsimony informative. Maximum parsimony analysis consisted of 1,439 constant characters; 308 informative characters and 450 variable characters parsimony-uninformative (Fig 2) (CI = 0.695, RI = 0.714, RC = 0.496, HI = 0.305). Maximum likelihood bootstrap values, maximum parsimony, and Bayesian posterior probability bootstrap values (MLBS/MPBS/BYPP) are given at nodes of the phylogram (Fig. 2). The phylogenetic tree inferred from the concatenated alignment resolved the six *Neopestalotiopsis* isolates from *Dypsis leptocheilos* and *Washingtonia robusta* into two distinct clades, representing an undermined species and new host record of *Neopestalotiopsis* (Fig. 2).

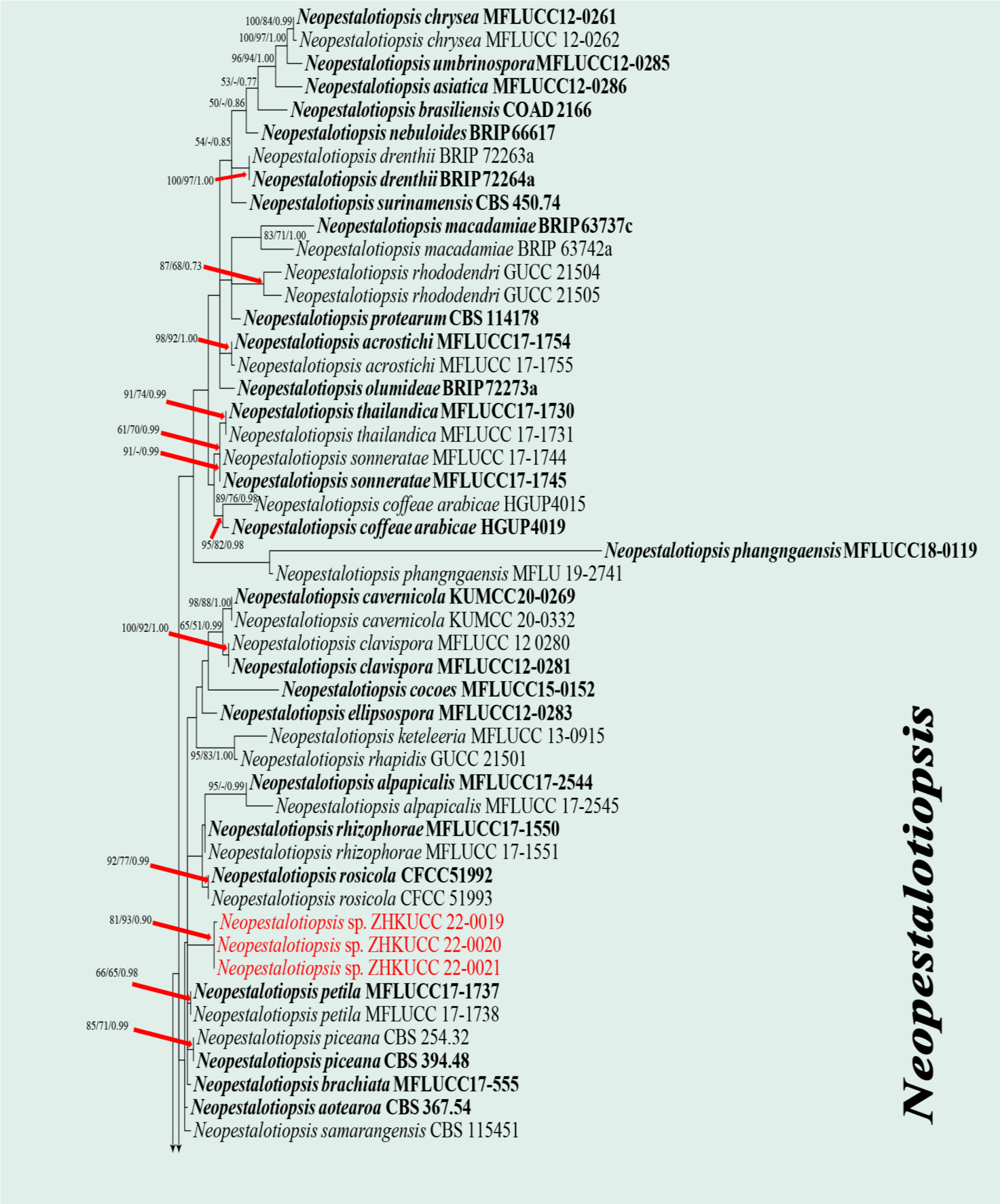

Fig. 2 – Phylogram generated from RAxML analysis based on combined ITS, *tub2* and *tef* 1-α sequence data of *Neopestalotiopsis* species. Bootstrap support values for maximum likelihood (ML) greater than 50 % and maximum parsimony (MP) greater than 50 % and Bayesian posterior probabilities (BYPP) greater than 0.60 are given at the nodes. The tree was rooted to *Pestalotiopsis diversiseta* (MFLUCC 12–0267) and *Pseudopestalotiopsis cocos* (CBS 272.29). The scale bar indicates 30.0 nucleotide changes per site. Isolates from this study are in red, and ex-type strains are in bold.

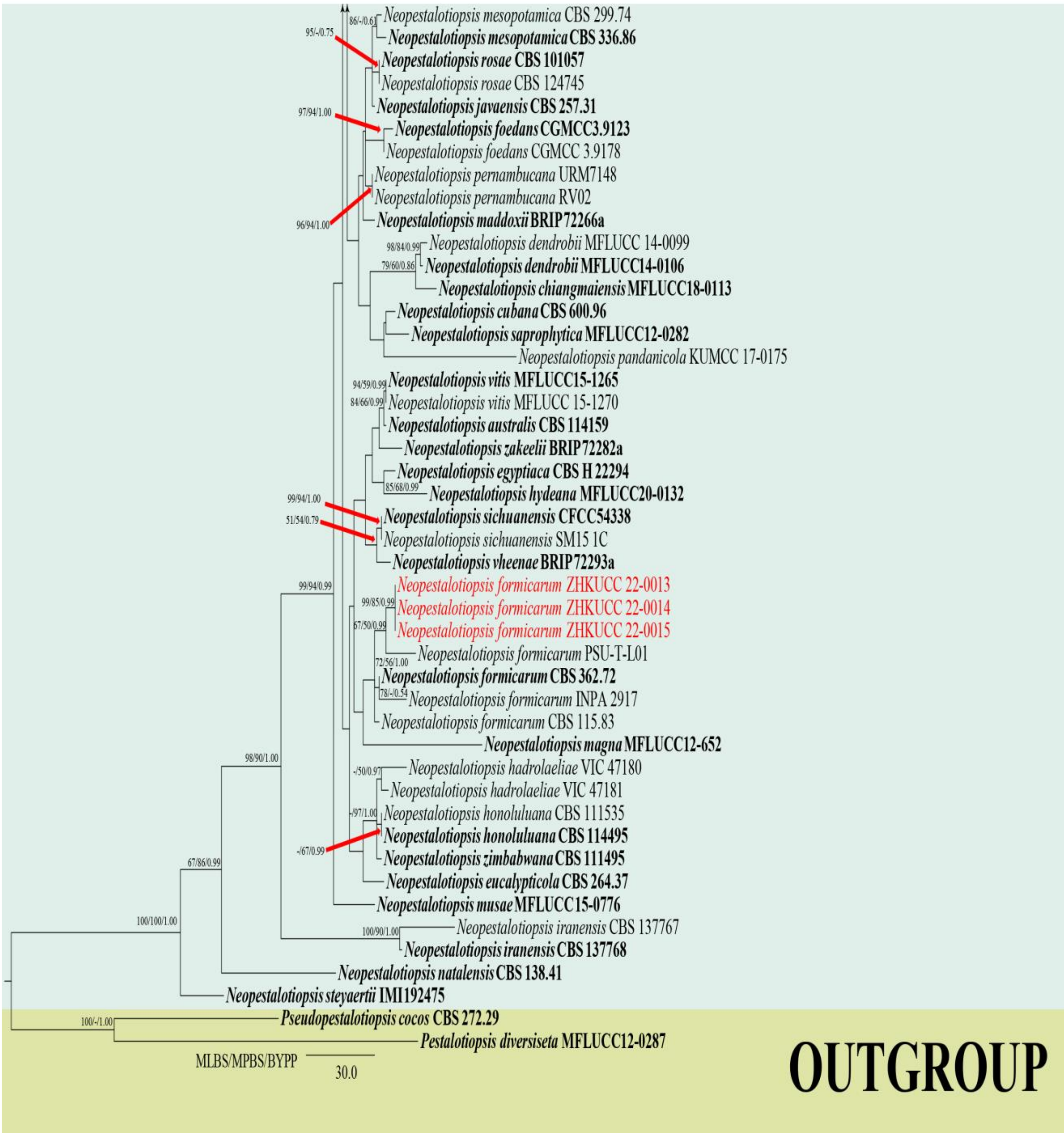

Fig. 2 – Continued.

Phylogenetic Analyses of *Pestalotiopsis*

The concatenated sequence data matrix of the phylogenetic tree comprised 2268 base pairs (bp) (508 for ITS, 416 for *tub2*, and 563 for *tef* 1-α). Similar tree topologies were obtained by ML, MP, and Bayesian analyses, and the best-scoring ML tree is shown in Fig. 3. The best-scoring ML tree had an optimization likelihood value of -10471.544238. The matrix had 654 distinct alignment patterns with an 11.01 % proportion of gaps and completely undetermined characters. Estimated base frequencies were as follows: A = 0.240175, C = 0.293350, G = 0.217702, T = 0.248772; substitution rates: AC = 0.923384, AG = 2.463554, AT = 1.031315, CG = 0.604015, CT = 4.228863, GT = 1.000000; gamma distribution shape parameter α = 0.280726. Incomplete portions at the ends of the sequences were excluded from the analysis. Maximum parsimony analysis yielded the best-scoring tree, of which 946 bp were constant, 193 bp were parsimony uninformative, and 348 bp parsimony informative. Maximum parsimony analysis consisted of 946 constant characters, 348 informative characters and 193 variable character parsimony-uninformative (Fig. 3) (CI = 0.523, RI= 0.808, RC = 0.423, HI = 0.477). Maximum likelihood bootstrap values, maximum parsimony, and Bayesian posterior probability bootstrap values (MLBS/MPBS/BYPP) are given at nodes of the phylogram (Fig. 3). The phylogenetic tree inferred from the concatenated alignment resolved the 22 *Pestalotiopsis* isolates from symptomatic *Areca triandra*, and *Arenga pinnata Sabal mexicana* into four monophyletic clades, representing the three new species and one new host record of *Pestalotiopsis* (Fig. 3).

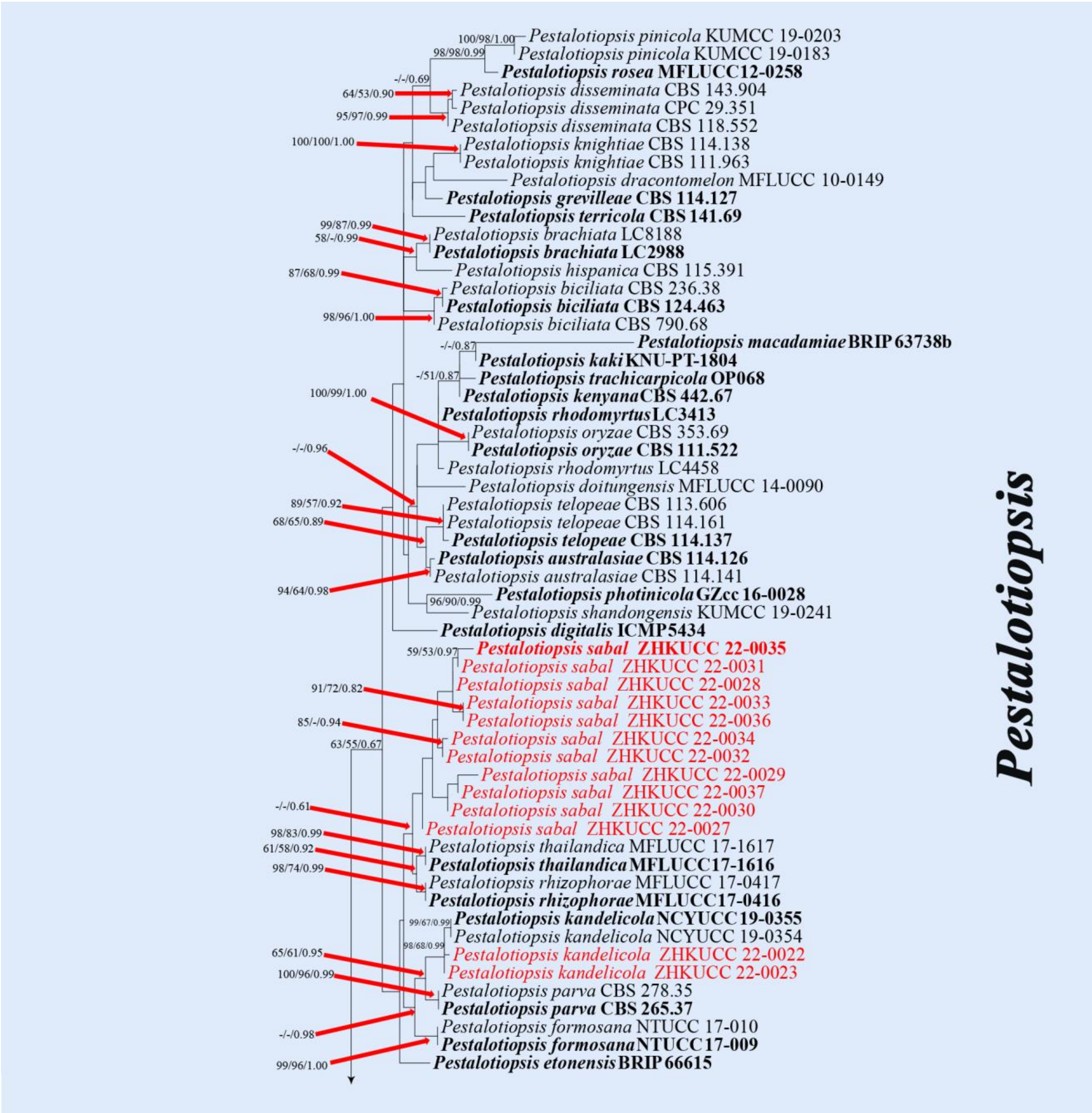

Fig. 3 – Phylogram generated from RAxML analysis based on combined ITS, *tub2* and *tef* 1-α sequence data of *Pestalotiopsis* species complex isolates. Bootstrap support values for maximum likelihood (ML) greater than 50 % and maximum parsimony (MP) greater than 50 % and Bayesian posterior probabilities (BYPP) greater than 0.60 are given at the nodes. The tree was rooted to *Neopestalotiopsis protearum* (CBS 114178) and *Pseudopestalotiopsis cocos* (CBS 272.29). The scale bar indicates 0.02 nucleotide changes per site. Isolates from this study are in red, ex-type strains are bold.

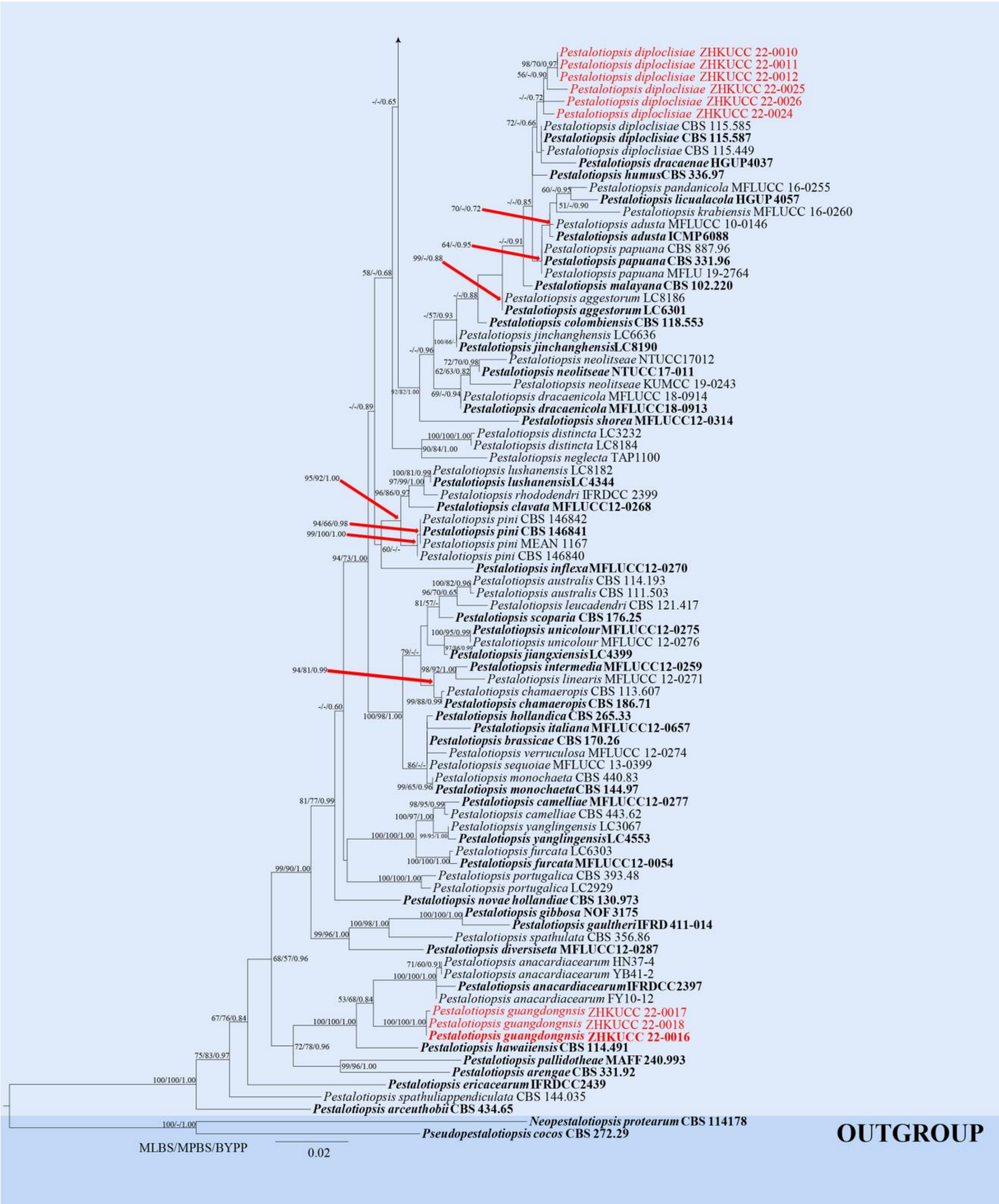

Fig. 3 – Continued.

PHI Analysis

In the phylogenetic analysis of *Pestalotiopsis* species, our isolates developed three distinct clades within the genus with low statistical support and significant tree lengths. Therefore, to confirm the species we conducted PHI analysis for these three clades. There was no evidence of significant genetic recombination ($Fw > 0.05$) between these novel species of *Pestalotiopsis* and the closely related species (Fig. 4). These results confirmed that these taxa are significantly different from the existing species of *Pestalotiopsis*.

In the phylogenetic analysis, Fig. 4a represents the split decomposition network of *Pestalotiopsis guangdongnsis* (ZHKUCC 22–0016) with four closely related taxa; *P*. *anacardiacearum* (IFRDCC 2397), *P*. *arengae* (CBS 331.92), *P*. *hawaiiensis* (CBS 114.491), *P*. *pallidotheae* (MAFF 240.993). There was no evidence of significant genetic recombination (Fw > 0.05) between *P*. *guangdongnsis* (ZHKUCC 22–0016) and other closely related species of *Pestalotiopsis*. The resulted split decomposition network of *P*. *sabal* (ZHKUCC 22–0035) with the five closely related taxa; *P*. *etonensis* (BRIP 66615), *P*. *formosana* (NTUCC 17–009), *P*. *kandelicola* (NCYUCC 19–0355), *P*. *rhizophroae* (MFLUCC 17–0416), *P*. *thailandica* (MFLUCC 17–1616) has also given no significant evidence of genetic recombination (Fw > 0.05) (Fig. 4b). Therefore, we identified them as novel *Pestalotiopsis* species from the palm.

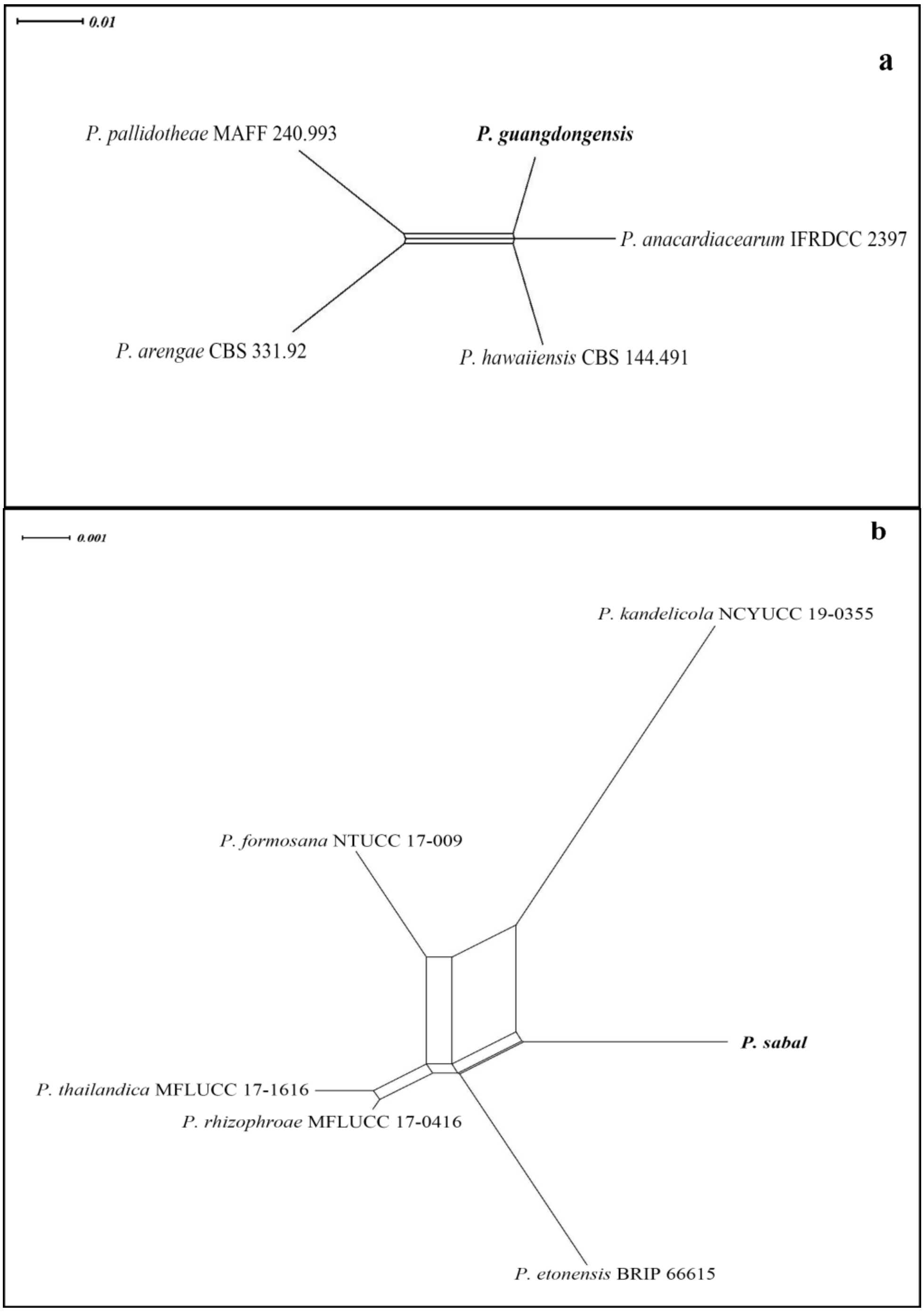

Fig. 4 – Split graphs show the results of the PHI test of (a) *Pestalotiopsis guangdongnsis* (Fw = 0.984). (b) *P*. *sabal* (Fw = 0.616) and their most closely related species using Log-Det transformation and split decomposition options. The new taxon in each graph is shown in bold font.

Taxonomy

Based on polyphasic approaches, six pestalotioid species were identified and characterized. Two *Neopestalotiopsis* species were identified as *N. formicidarum* and *Neopestalotiopsis* sp. There are four *Pestalotiopsis* species, namely *P. areca*, *P. guangdongensis*, *P. kandelicola* and *P. sabal*. For all these identified taxa, species descriptions and illustrations were given below. A comparison of morphological data of the species identified in this study with their closely related species in the phylogenetic analysis is shown in Table 3. The comparison results in Table 3 are consistent with the phylogenetic analysis and the results of PHI. The conidial characters *N. formicidarum* (ZHKUCC 22–0013) and *N. formicidarum* (CBS 362.72) are almost identical; *P. kandelicola* (ZHKUCC 22–0022) similar to the conidial morphology of *P. kandelicola* (NCYUCC 19–0355) and *P. diploclisiae* (ZHKUCC 22–0010), similar to the conidial morphology of *P. diploclisiae* (CBS 115587). However, the conidia of *P. guangdongensis* (ZHKUCC 22–0016) and *P. hawaiiensis* (CBS 114491) are quite different in the sizes of basal cells, median cells and apical cells are different. This is also the case for *P. sabal* (ZHKUCC 22–0035) and *P. thailandica* (MFLUCC 17–1616).

Table 3 Comparison of conidia of sister clade species related to this study.

Species	Conidia size (µm)	Basal cell (µm)	Basal appendage		Three median cells (µm)				Apical cell (µm)	Apical appendages	
			Number	Length (µm)	Sum of three median cells	second	third	fourth		Number	Length (µm)
Neopestalotiopsis brachiate (LC2988)	(20–)21–26.5(–27.5) × (4.7–)5.5–6(–6.3)	(3–)3.5–4(–5)	1	(3.5–)4–9(–10)	(10–)10.5–15(–16)	(3–)4–5 (–6)	(3.5–)4–5 (–6)	(3–)4–5(–5.5)	(4–)4.5–5(–6)	1–3	(8.5–)9.5–33(–34)
N. formicidarum (CBS 362.72)	(20–)21–28(–29) × 7.5–9.5	4.5–6	1	4–8	(14–)15–16.5(–17)	4–6.5	4–6	4.5–6.5	4–5.5	2–3	(20–)23–33(–36)
N. formicidarum (ZHKUCC 22–0013)	20–25 × 7–8	3–6	1	2.5–6	13–16	4–6.5	4–6	4.5–6	3–4.5	1–3	16–26
N. magna (MFLUCC 12–652)	(40)42–46(47) × (9)9.5–12	8.5–9	1	11–15	(30)31–33.5(34)	9.5–11.5	9.5–11	10.5–12	5–8	2–4	(10)16–26(30)
N. petila (MFLUCC 17–1737)	(20–)21–26.5(–27.5) × (5.6–)6–7(–7.8)	(3–)4–5.5(–6)	1	(2–)3–8 (–9)	(12. 5–)13. 5–15(–17)	(4.5–)5–6 (–7)	(3.5–)4–5 (–5.5)	(4.5–)5–5.5(–6)	(3–)4–5(–7)	2–3	(21–)22–29(–33)
N. phangngaensis (MFLUCC 18–0119)	18–25 × 6–7.5	3–5	1	3–6	13–15	3.5–5	2.5–5	4–5	3–4.5	3	16–24.5
N. sichuanensis (CFCC 54338)	(23.2–)24.3–30.4(–32.8) × (5.7–)6.3–7.1(–7.5)	3.5–5	1	1.5–4	NA	3.5–6	4.5–6.5	4.5–6	3.5–6	2–3	8–15
N. sp. (ZHKUCC 22–0019)	22–27 × 6–9	2–6	1	2–4.5	15–18	5–6.5	5–6	5–7	2.5–5	1–3	3–15
Pestalotiopsis anacardiacearum (IFRDCC 2397)	27–39 × 7–10	5–7.5	1	5–9	19–22	6.5–8.5	6.8–7.5	6.7–8.5	4–5.3	2–3	20–45

Table 3 Continued.

Species	Conidia size (µm)	Basal cell (µm)	Basal appendage		Three median cells of conidia (µm)				Apical cell (µm)	Apical appendages	
			Number	Length (µm)	Sum of three median cells	second	third	fourth		Number	Length (µm)
P. diploclisiae (ZHKUCC 22–0010)	16–25 × 5–6	3.5–6	1	4–8.5	10–15	4–5.5	3.5–5	3.5–6	3–6	1–3	8–20
P. diploclisiae (CBS 115587)	(20–)22–26.5(–28) × 5–6.5(–7)	4–6.5	1	3–8	(13.5–)14–16(–17)	4.5–6	4.5–7	4.5–6.5	3.5–6	2–4	(10–)13–19(–22)
P. dracaenae (HGUP4037)	18–24 × 6.5–8.5	3–4.5	1	3–7	11.5–16	3.5–5.5	4–5.5	4–5.5	3–5.5	2–4	6.5–15.5
P. formosana (NTUCC 17–009)	(15–)18–22(–26) × (5–)6–7	(3–)4–5(–6)	1	(2–)3–5(–6)	(10–)11–14(–16)	(3–)4–5(–6)	3–4(–5)	(3–)4–5	(2–)3–4	2–3	(8–)11–16(–20)
P. guangdongensis (ZHKUCC 22–0016)	27–39 × 8–11	4–8	1	2–13	20–26	6–8	7–10	7–10	4.5–7	1–4	12–43
P. hawaiiensis (CBS 114491)	(26–)27–34.5(–37) × (7–)7.5–10(–10.5)	4–8	1	5–11	(19–)19.5–23(–25)	5–8.5	6.5–9.5	6–9	4–7	2–3	(14–)19–33(–36)
P. humus (CBS 336.97)	(17–)18.5–22(–23) × 5–7(–7.5)	3.5–5.5	1	2–5	(11.5–)12–14(–14.5)	3.5–5.5	3.5–6	3.5–5.5	3.5–4.5	2–3	(6–)6.5–12(–13)
P. kandelicola (NCYUCC 19–0355)	20–23.5 × 4–6	(3–)3.5–4.5(–5)	1	(2–)2.5–3(–3.5)	(12–)13–14(–15)	(3–)3.5–4(–5)	(3–)4–5(–6)	(3–)4–5(–6)	(3–)3.5–4(–4.5)	2–3	(11–)13–14(–15)
P. kandelicola (ZHKUCC 22–0022)	17.5–22 × 5.5–7	3.5–5	1	2.5–6	10–13	4–5	3.5–4.5	4–5	3.5–5	1–3	9–28
P. parva (CBS 265.37)	(16–)16.5–20(–21) × 5–7(–7.5)	3–5	1	2–4	(10–)10.5–13(–13.5)	3.5–5	3.5–4.5	4–5	(2–)2.5–4	2–3	(6–)6.5–12(–13)
P. rhizophorae (MFLUCC 17–0416)	(17–)17.5–23(–23.5) × (5.5–)6–6.5(–7)	(2–)3–3.5(–5)	1	1.5–4.5(–5)	(11–)11.5–14(–14.5)	(3.5–)4–5(–5.5)	(3–)4–4.5(–5)	(3.5–)4–5(–5.5)	(1.8–)2–3(–4.5)	1–2	(7.5–)8–13(–14.5)
P. sabal (ZHKUCC 22–0035)	17.5–23 × 5.5–7	3–5.5	2	3–6	11–14	3–5	3.5–5	3.5–5	3–5	1–3	7–20
P. thailandica (MFLUCC 17–1616)	(17–)17.5–28(–29) × (4.9–)5.5–6.5(–7.1)	(1.8–)2–4(–6)	1	(2–)2.5–9.5(–10)	(12–)12.5–16(–18)	(4–)4.5–6(–7)	(3.5–)4–4.5(–5.5)	(3.5–)4–5(–6.5)	(2–)3.5–4(–6)	1–2	(5.5–)11–34(–38)

Neopestalotiopsis Taxonomy

Neopestalotiopsis formicidarum Maharachch., K.D. Hyde & Crous [as 'formicarum'], in Maharachchikumbura, Hyde, Groenewald, Xu & Crous, Stud. Mycol. 79: 140 (2014). Fig. 5

Index Fungorum number: IF821673; Facesoffungi number: FoF10804

Conidiomata erumpent or superficial, oval or hemispherical, irregular, scattered or aggregate, with the stromata surface slightly convex or slightly flat. *Conidiophores* reduced to conidiogenous cells, smooth, hyaline. *Conidiogenous cells* 5.5 × 3.5 µm, discrete, thin-walled, hyaline, lageniform, sub-cylindrical or irregular, proliferating 1–3 times percurrently. *Conidia* 20–25 × 7–8 µm ($\bar{x}$ ± SD = 22 ± 1.9 × 7.5 ± 0.5 µm, n = 40),fusiform to ellipsoidal, 4-septate, straight to slightly curved; basal cell 3–6 µm long obconic with a truncate base, hyaline, minutely verruculose and thin-walled; three median cells 13–16 µm long ($\bar{x}$ ± SD = 14.4 ± 1 µm), doliiform, smooth, concolourous, olivaceous, septa darker than the rest of the cell (second cell from the base 4–6.5 µm; third cell 4–6 µm; fourth cell 4.5–6 µm); apical cell 3–4.5 µm long, hyaline, conical to subcylindrical, smooth, thin-walled; apical appendages 16–26 µm long, ($\bar{x}$ ± SD = 21.2 ± 2.7 µm), 1–3 (seldom 1), tubular, arising from the apical crest, unbranched, filiform; basal appendage, 2.5–6 µm long single, tubular, unbranched, centric.

Teleomorph – Not observed.

Known distribution – widespread in tropical and subtropical regions.

Material examined – CHINA, Guangdong Province, Guangzhou City, South China Botanical Garden, rotting tree axis of *Dypsis leptocheilos*, 30 November 2020, Y.R. Xiong, ZHKUCC 22–0013 (ZHKU 22–0010, new host record) – living culture in ZHKUCC; *ibidem*, 30 November 2020, Y.R. Xiong, ZHKUCC 22–0014 (paratype) – living culture in ZHKUCC; 30 November 2020, Y.R. Xiong, ZHKUCC 22–0015 (paratype) – living culture in ZHKUCC.

Notes – In the present study three isolates obtained from *Dypsis leptocheilos* clustered together with *Neopestalotiopsis formicidarum* (CBS 362.72) with 67% ML, 50% MP bootstrap values and 0.99 BYPP value. *Neopestalotiopsis formicidarum* was originally described from dead ants in Ghana and plant debris from Cuba (Maharachchikumbura et al. 2014). Isolates obtained in this study are morphologically similar to the original description of *N. formicidarum* (Maharachchikumbura et al. 2014). Therefore, based on morphology and DNA new data (Fig. 2), we identified *N. formicidarum* isolates ZHKUCC 22–0013 as a novel host record on *Dypsis leptocheilos* from China.

***Neopestalotiopsis* sp.** Fig. 6

Conidiomata stromatic, acervulus, semi–immersed, beneath pale, erumpent and raised areas of host epidermis, central black ostioles, scattered or aggregate, spores scattered around the dehisce. *Conidiophores* reduce to conidiogenous cells, smooth, hyaline. *Conidiogenous cells* 13 × 6.5 µm, discrete, cylindrical to sub-cylindrical, smooth-walled, hyaline. *Conidia* 22–27 × 6–9 µm ($\bar{x}$ ± SD = 24 ± 1.6 × 7.5 ± 1 µm, n = 40), fusoid, ellipsoidal to subcylindrical, 4-septate, straight to slightly curved; basal cell 2–6 µm long, semiellipsoid to obconic, or ampulliform, with a truncate base, hyaline, minutely verruculose and smooth-walled; three median cells 15–18 µm long, $\bar{x}$ ± SD = 17 ± 1 µm, doliiform, versicolored, brown to pale brown, septa darker than the rest of the cell (second cell from the base 5–6.5 µm; third cell 5–6 µm; fourth cell 5–7 µm); apical cell 2.5–5 µm long, hyaline, conical to subcylindrical, smooth, thin- and smooth-walled; apical appendages 3–15 µm long, $\bar{x}$ ± SD = 6.5 ± 2.8 µm, 1–3, tubular, arising from the apical crest, unbranched, filiform; basal appendage 2–4.5 µm long, single, tubular, unbranched, centric.

Teleomorph – Not observed.

Known distribution – widespread in tropical and subtropical regions.

Material examined – CHINA, Yunnan Province, Kunming City, Kunming Institute of Botany CAS, from rotting branches of the *Washingtonia robusta*, 7 May 2021, Y.R. Xiong, ZHKUCC 22–0019 (ZHKU 22–0012, holotype) – living culture in ZHKUCC; *ibidem*, 7 May 2021, Y.R. Xiong, ZHKUCC 22–0020 (paratype) – living culture in ZHKUCC; 7 May 2021, Y.R. Xiong, ZHKUCC 22–0021 (paratype) – living culture in ZHKUCC.

Notes – Three isolates from our collection developed an independent clade in the phylogenetic tree with 81% ML, 93% MP bootstrap values and 0.90 BYPP value. *Neopestalotiopsis* sp. was phylogenetically close to *N. brachiata*, *N. petila* and *N. piceana*. The conidia of *Neopestalotiopsis* sp. and *N. petila* are similar in morphology but different in size, as shown in Table 3. *Neopestalotiopsis* sp. has 1–3 apical appendages, and *N. petila* has 2–3. However, according to phylogenetic analysis and morphology, isolates were not assigned to any new taxa and were tentatively placed into one clade following Gerardo-Lugo et al. (2020).

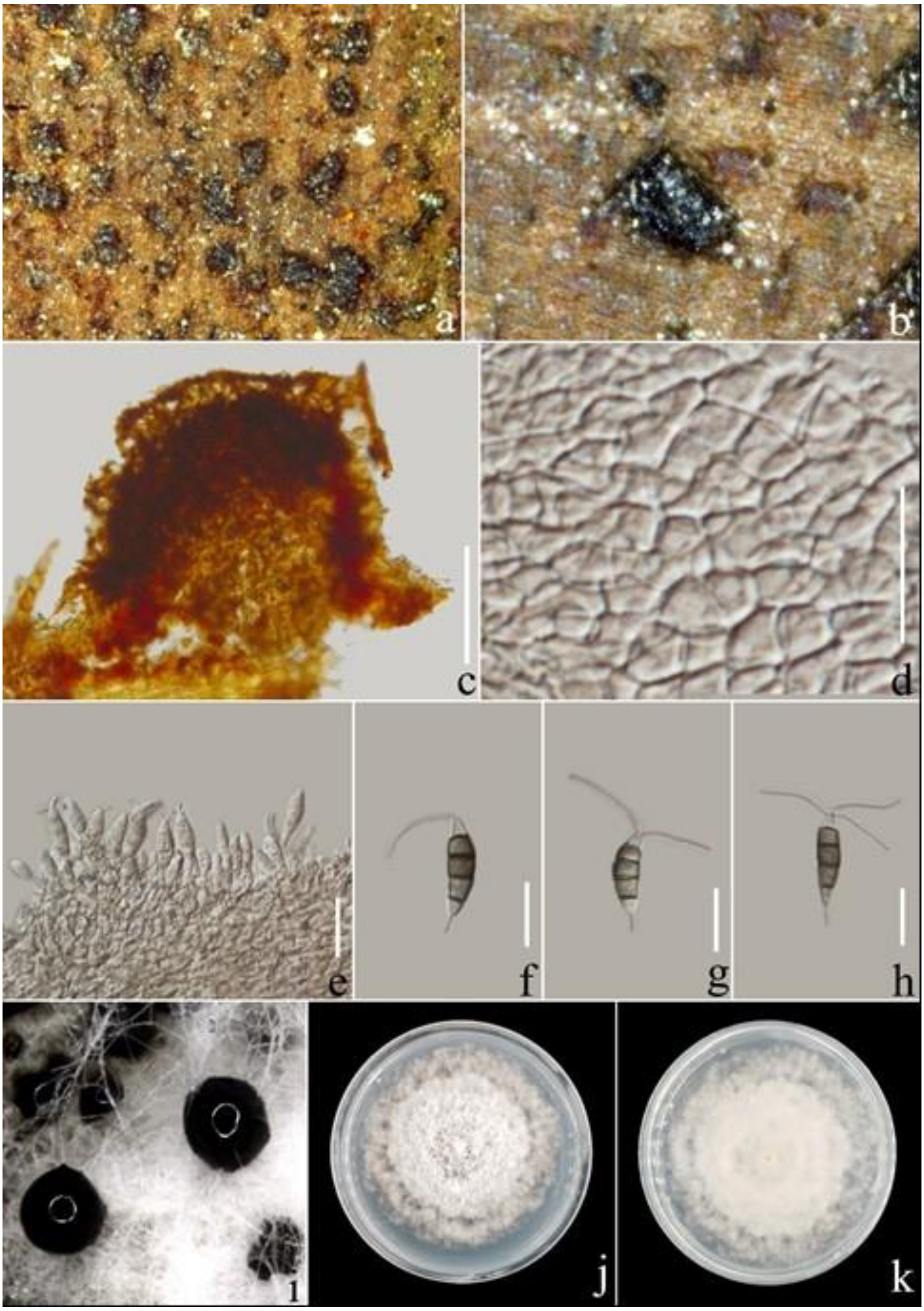

Fig. 5 – *Neopestalotiopsis formicidarum*. ZHKU 22–0010. a, b Conidiomata on the rotting axis of Dypsis leptocheilos. c, d Peridium. e Conidiogenous cells give rise to conidia. f–h Conidia. i Pycnidium. j The top view of a two-week-old colony on PDA. k The bottom view of a two-week-old colony on PDA. Scale bars: c = 50 µm; d = 15 µm; e = 20 µm; f–h = 15 µm.

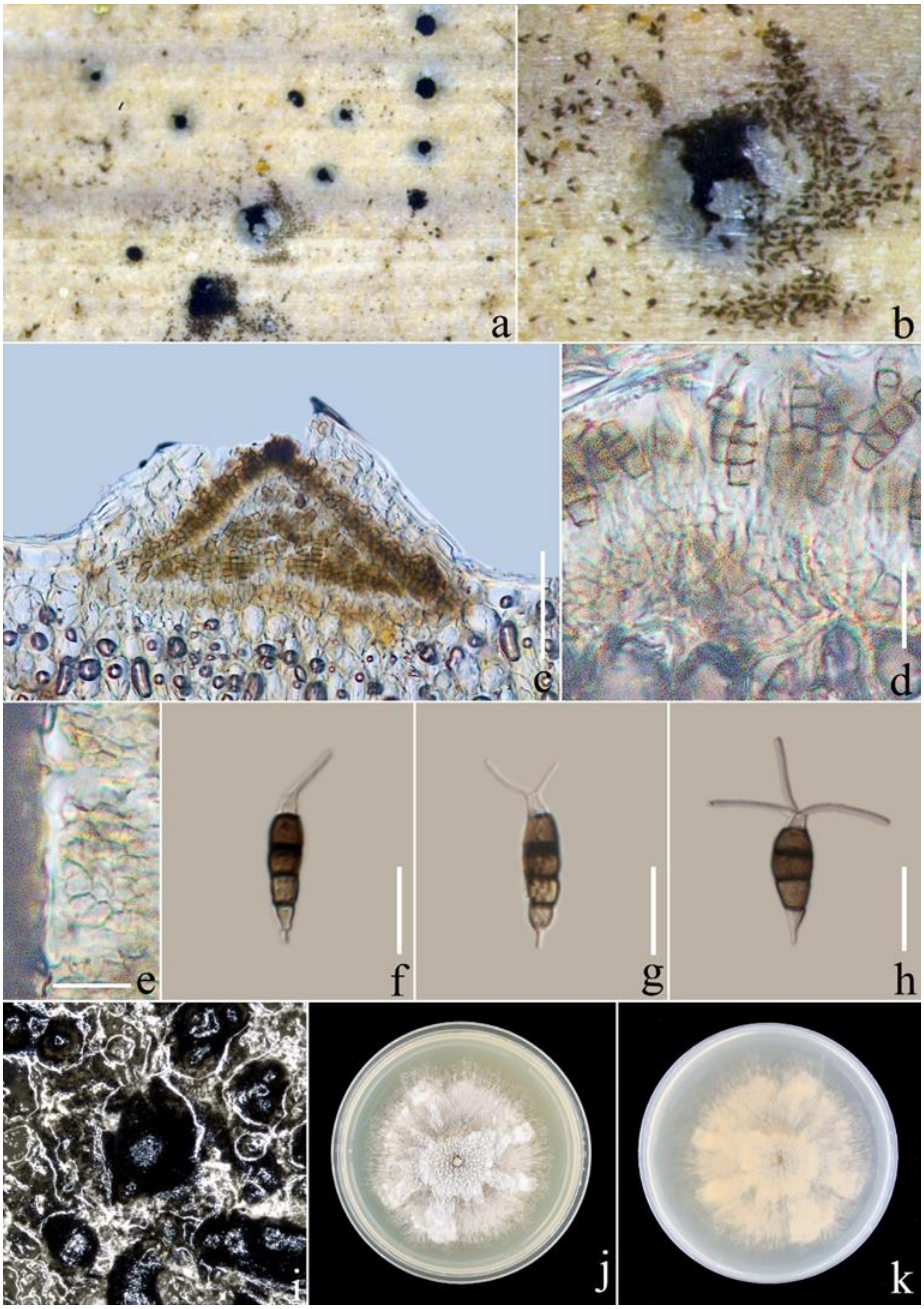

Fig. 6 – *Neopestalotiopsis* sp. ZHKU 22–0012. a, b Conidiomata on the rotting branches of *Washingtonia robusta*. c, e Peridium. d Conidiogenous cells give rise to conidia. f–h Conidia. i Pycnidia. j The top view of a two-week-old colony on PDA. k The bottom view of a two-week-old colony on PDA. Scale bars: c = 50 µm, d–h = 15 µm.

Pestalotiopsis Taxonomy

Pestalotiopsis diploclisiae Maharachch., K.D. Hyde & Crous, Stud. Mycol. 79: 140 (2014).

Fig. 7

Index Fungorum number: IF809737

Conidiomata stromatic, acervulus, erumpent, immersed under a host epidermal clypeus, raising host surface and producing a dark brown area of dehiscence, scattered. *Conidiophores* sparsely septate, unbranched or branched at the base, irregular, hyaline, up to 15 µm long. *Conidiogenous cells* 5 × 2 µm, discrete, smooth-walled, hyaline, sparsely verruculose, lageniform or sub-cylindrical. *Conidia* 16–25 × 5–6 µm ($\bar{x}$ ± SD = 23 ± 2.6 × 6 ± 0.5 µm, n = 40), fusiform to ellipsoidal, 4-septate, straight to slightly curved; basal cell 3.5–6 µm long, conic with a truncate base, hyaline, minutely verruculose, thin- and smooth-walled; three median cells 10–15 µm long, $\bar{x}$ ± SD = 14 ± 1.4 µm, doliiform, smooth, concolourous, olivaceous, septa darker than the rest of the cell (second cell from the base 4–5.5 µm; third cell 3.5–5 µm; fourth cell 3.5–6 µm); apical cell 3–6 µm long, hyaline, conical to subcylindrical, smooth-walled; apical appendages 8–20 µm long, $\bar{x}$ ± SD = 14.5 ± 3.5 µm, 1–3 (most 2), tubular, arising from the apical crest, unbranched, filiform; basal appendage 4–8.5 µm long, single, tubular, unbranched, centric.

Teleomorph – Not observed.

Known distribution – widespread in tropical and subtropical regions.

Material examined – CHINA, Guangdong Province, Shenzhen City, Fairy Lake Botanical Garden, rotting tree axis of the *Areca triandra*, 30 November 2020, Y.R. Xiong, ZHKUCC 22–0010 (ZHKU 22–0009, new host record) – living culture in ZHKUCC; *ibidem*, 30 November 2020, Y.R. Xiong, ZHKUCC 22–0011 (paratype) – living culture in ZHKUCC; 30 November 2020, Y.R. Xiong, ZHKUCC 22–0012 (paratype) – living culture in ZHKUCC. CHINA, Guangdong Province, Guangzhou City, South China Botanical Garden, symptomatic lamina of *Sabal mexicana*, 17 June 2020, Y.R. Xiong, ZHKUCC 22–0024 (paratype) – living culture in ZHKUCC; 17 June 2020, Y.R. Xiong, ZHKUCC 22–0025 (paratype) – living culture in ZHKUCC.

Notes – In the present study three isolates obtained from *Areca triandra* clustered together with *Pestalotiopsis diploclisiae* with 72% ML values and 0.66 BYPP value. *Pestalotiopsis diploclisiae* was originally described from fruits of *Diploclisia glaucescens* and *Psychotria tutcheri* from China (Maharachchikumbura et al. 2014). Isolates obtained in this study are morphologically similar to the original description of *P. diploclisiae* (Maharachchikumbura et al. 2014). Therefore, based on morphology and new DNA data (Fig. 2), we identified *P. diploclisiae* isolates as a novel host record on *A. triandra* from China.

Pestalotiopsis guangdongensis Y.R. Xiong & Manawas., sp. nov. Fig. 8

Index Fungorum number: IF559616; Facesoffungi number: FoF10805

Etymology – Epithet refers to the locale from where the fungus was isolated.

Holotype – ZHKU 22–0011

Conidiomata immersed beneath inconspicuous, intra- or sub-epidermal, ellipsoidal domes on the host surface, black, coriaceous, scattered. *Conidiophores* mostly reduced to conidiogenous cells, branched or unbranched, circular, hyaline, smooth-walled, up to 7.5 µm long. *Conidiogenous cells* 5.5 × 7 µm, discrete, smooth-walled, hyaline, ampulliform or sub-cylindrical. *Conidia* 27–39 × 8–11 µm ($\bar{x}$ ± SD = 33.5 ± 3.6 × 9.6 ± 0.8 µm, n = 40), fusoid, ellipsoid, 4-septate, straight to slightly curved, slightly constricted at septa; basal cell 4–8 µm long, conic with a truncate base, hyaline, verruculose and thin-walled; three median cells 20–26 µm long, $\bar{x}$ ± SD = 22.5 ± 2 µm, doliiform, verruculose, concolourous, olivaceous, septa darker than the rest of the cell (second cell from the base 6–8 µm; third cell 7–10 µm; fourth cell 7–10 µm); apical cell 4.5–7 µm long, hyaline, verruculose, subcylindrical to conical, smooth-walled; apical appendages 12–43 µm long, $\bar{x}$ ± SD = 28 ± 7 µm, 1–4 (seldom 4), tubular, arising from the apical crest, unbranched, filiform; basal appendage 2–13 µm long, single, tubular, unbranched, centric.

Teleomorph – Not observed.

Known distribution – widespread in tropical and subtropical regions.

Material examined – CHINA, Guangdong Province, Guangzhou City, South China Botanical Garden, rotting leaf of *Arenga pinnata*, 17 December 2020, Y.R. Xiong, ZHKUCC 22–0016 (ZHKU 22–0011, holotype) – living culture in ZHKUCC; *ibidem*, 17 December 2020, Y.R. Xiong, ZHKUCC 22–0017 (paratype) – living culture in ZHKUCC; 17 December 2020, Y.R. Xiong, ZHKUCC 22–0018 (paratype) – living culture in ZHKUCC.

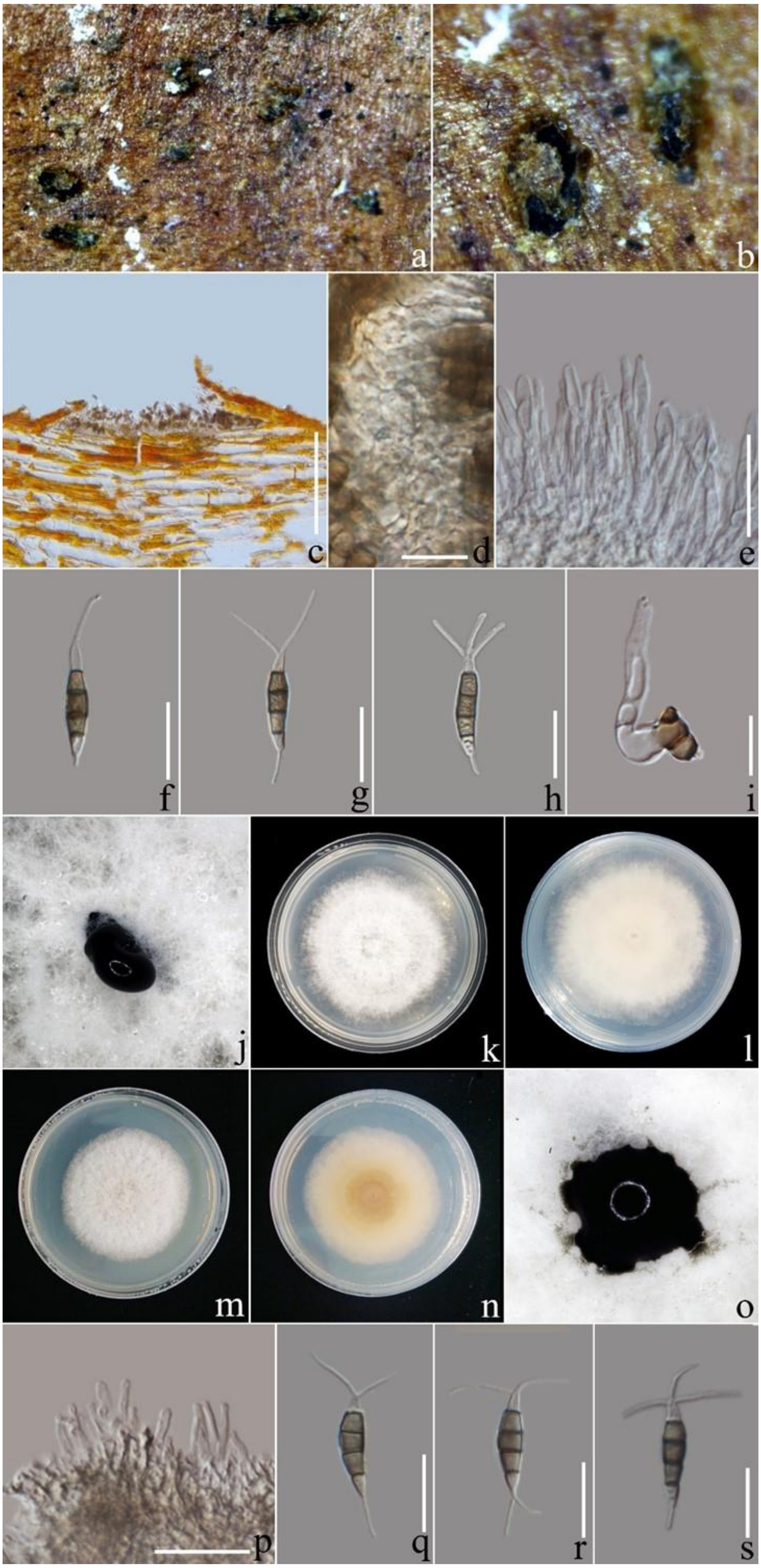

Fig. 7 – *Pestalotiopsis diploclisiae*. ZHKU 22–0009. a, b Conidiomata on the rotting axis of *Areca triandra*. c, d Peridium. e Conidiogenous cells give rise to conidia. f–h Conidia. i Germinating

conidia. j Pycnidium. k The top view of a two-week-old colony on PDA. l The bottom view of a two-week-old colony on PDA. m The top view of a two-week-old colony on PDA from pathogenic samples. n The bottom view of a two-week-old colony on PDA from pathogenic samples. o Pycnidium from pathogen. p Conidiogenous cells give rise to conidia. q–s Conidia from pathogen. Scale bars: c = 100 µm, d = 10 µm, e = 20 µm, f–i = 15 µm, p = 20 µm, q–s = 15 µm.

Fig. 8 – *Pestalotiopsis guangdongensis*. ZHKU 22–0011. a, b Conidiomata on the rotting axis of *Arenga pinnata*. c Peridium. d Conidiogenous cells give rise to conidia. e–i Conidia. j Pycnidium. (k) The top view of a two-week-old colony on PDA. (l) The bottom view of a two-week-old colony on PDA. Scale bars: c = 20 µm, d–h = 30 µm, i = 15 µm.

Notes – Three isolates obtained in this study from an independent clade in *Pestalotiopsis* phylogenetic tree with 53 % ML, 68 % MP bootstrap values and 0.84 BYPP values. *Pestalotiopsis* *guangdongensis* was phylogenetically close to *P. anacardiacearum*, and *P. hawaiiensis*. *Pestalotiopsis guangdongensis* have 1–4 apical appendages, and *P. anacardiacearum* has 2–3. Although the size of the conidia of *P. guangdongensis* is similar to that of *P. anacardiacearum*, the sizes of basal cells, median cells and apical cells are different (Table 3). In addition, there is no evidence of significant genetic recombination (Fw = 1.0) in the PHI analysis. Based on polyphasic approaches, the isolates obtained in this study was identified as *P. guangdongensis*, a new *Pestalotiopsis* species.

Pestalotiopsis kandelicola Norph., C.H. Kuo & K.D. Hyde, Fungal Diversity. 103:219–271 (2020b). Fig. 9

Index Fungorum number: IF557755; Facesoffungi number: FoF08934

Conidiomata 395–425 µm diam, pycnidial in culture on PDA, globose to clavate, solitary or aggregate, black, semi-immersed, ostiole in the center; releasing conidia in a black, slimy, globose, glistening mass. *Conidiophores* sparsely septate at base, hyaline, subrotund to irregular, branched or unbranched, up to 15.5 µm. *Conidiogenous cells* 4 × 2 µm, discrete, smooth-walled, hyaline, ampulliform to subcylindrical. *Conidia* 17.5–22 × 5.5–7 µm ($\bar{x}$ ± SD = 20 ± 1.3 × 6 ± 0.5 µm, n = 40), fusiform to ellipsoid, 4-septate, straight to slightly curved, slightly constricted at septa; basal cell 3.5–5 µm long, conic with a truncate base, hyaline, sparsely verruculose and thin-walled; three median cells 10–13 µm long, $\bar{x}$ ± SD = 12 ± 1 µm, doliiform, verruculose, concolourous, maple, septa darker than the rest of the cell (second cell from the base 4–5 µm; third cell 3.5–4.5 µm; fourth cell 4–5 µm); apical cell 3.5–5 µm long, hyaline, sparsely verruculose, conical to subcylindrical, thin- or smooth-walled; apical appendages 9–28 µm long, $\bar{x}$ ± SD = 16.5 ± 4.3 µm, 1–3 (seldom 1), tubular, arising from the apical crest, unbranched, filiform; basal appendage 2.5–6 µm long, single, tubular, unbranched, centric.

Teleomorph – Not observed.

Known distribution – widespread in tropical and subtropical regions.

Material examined – CHINA, Guangdong Province, Guangzhou City, South China Botanical Garden, symptomatic lamina of *Sabal mexicana*, 17 June 2020, Y.R. Xiong, ZHKUCC 22–0022 (ZHKU 22–0013, new host record) – living culture in ZHKUCC; *ibidem*, 17 June 2020, Y.R. Xiong, ZHKUCC 22–0023 (paratype) – living culture in ZHKUCC.

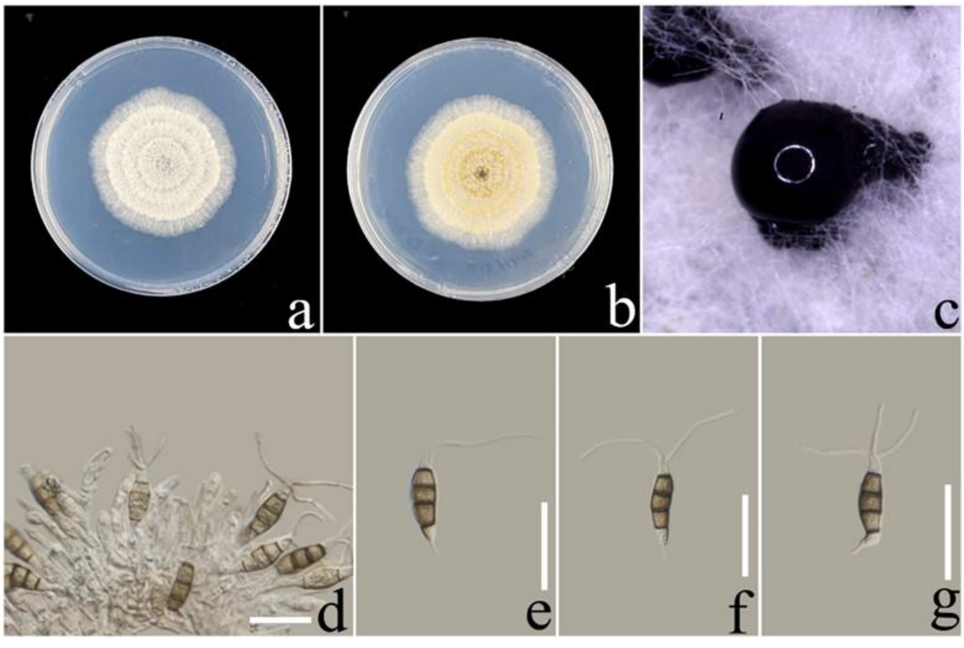

Fig. 9 – *Pestalotiopsis kandelicola*. ZHKU 22–0013. a The top view of a two-week-old colony on PDA. b The bottom view of a two-week-old colony on PDA. c Pycnidium. d Conidiogenous cells give rise to conidia. e–g Conidia. Scale bars = 15 µm.

Notes – The two isolates obtained in this study (ZHKUCC 22–0022, ZHKUCC 22–0023) develop an independent clade in *Pestalotiopsis* phylogenetic tree with 98% ML, 68% MP bootstrap values and 0.99 BYPP value. *Pestalotiopsis kandelicola* was reported on *Kandelia candel* (*Rhizophoraceae*), Taiwan (Hyde et al. 2020b). The present study adds *Sabal mexicana* as a new host for this fungus based on the phylogenetic inference of ITS, *tub2*, *tef* 1-α sequence data (Fig. 3), and morphology (Table 3).

Pestalotiopsis sabal Y.R. Xiong & Manawas., sp. nov. Fig. 10

Index Fungorum number: IF559618; Facesoffungi number: FoF10806

Etymology – Epithet refers to the host genus from which the fungus was isolated.

Holotype – ZHKU 22–0035

Conidiomata 490–560 µm diam, pycnidial (on PDA), globose to clavate, solitary or aggregate, black, semi-immersed, ostiole in the center; releasing conidia in a black, slimy, globose, glistening mass. *Conidiophores* reduce to conidiogenous cells, smooth, hyaline. *Conidiogenous cells* 4.5 × 3 µm, discrete, smooth-walled, hyaline, subcylindrical. *Conidia* 17.5–23 × 5.5–7 µm ($\bar{x}$ ± SD = 20 ± 1.7 × 6.5 ± 0.6 µm, n = 40), fusiform to ellipsoid, 4-septate, slightly constricted at septa, straight to slightly curved; basal cell 3–5.5 µm long, conic with a truncate base, hyaline, sparsely verruculose and thin- or smooth-walled; three median cells 11–14 µm long, $\bar{x}$ ± SD = 12 ± 1 µm, doliiform, sparsely verruculose, versicolored, olivaceous, septa darker than the rest of the cell (second cell from the base 3–5 µm; third cell 3.5–5 µm; fourth cell 3.5–5 µm); apical cell 3–5 µm long, hyaline, sparsely verruculose, conical to subcylindrical, smooth-walled; apical appendages 7–20 µm long, $\bar{x}$ ± SD = 14 ± 3.4 µm, 1–3 (seldom 1), tubular, arising from the apical crest, unbranched, filiform; basal appendage 3–6 µm long, 1–2, tubular, unbranched, centric.

Teleomorph – Not observed.

Known distribution – widespread in tropical and subtropical regions.

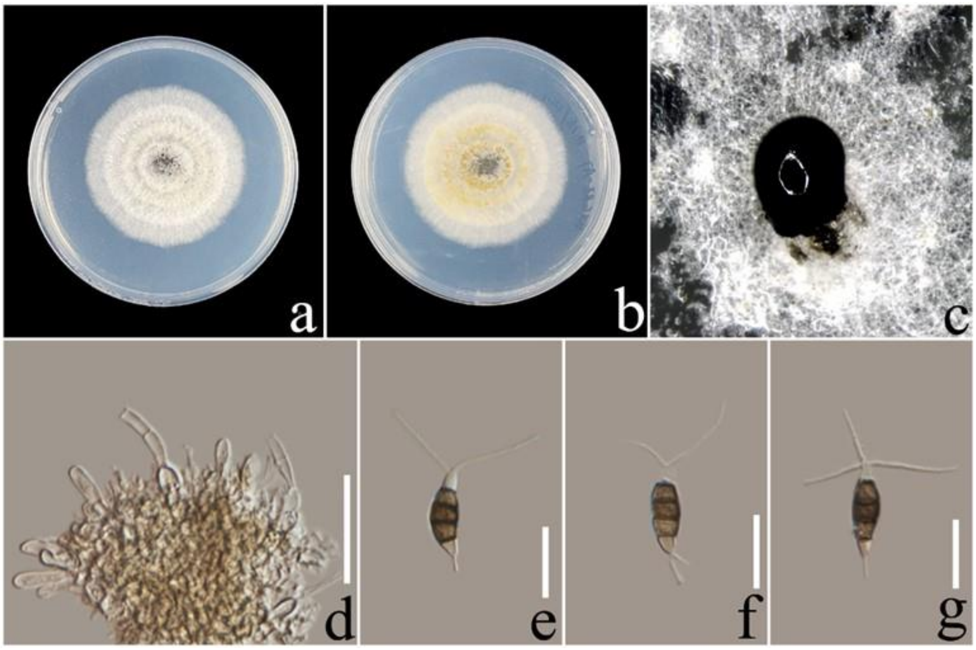

Fig. 10 – *Pestalotiopsis sabal*. ZHKU 22–0035. a The top view of a two-week-old colony on PDA. b The bottom view of a two-week-old colony on PDA. c Pycnidium. d Conidiogenous cells give rise to conidia. e–g Conidia. Scale bars: d = 30 µm, e–g = 15 µm.

Material examined – CHINA, Guangdong Province, Guangzhou City, South China Botanical Garden, symptomatic lamina of *Sabal mexicana*, 17 June 2020, Y.R. Xiong, ZHKUCC 22–0026 (ZHKU 22–0035, holotype as dry culture) – living culture in ZHKUCC; Additional herbarium materials ZHKU 22–0019 to ZHKU 22–0028 (dry cultures); living cultures ZHKUCC 22–0027, ZHKUCC 22–0028, ZHKUCC 22–0029, ZHKUCC 22–0030, ZHKUCC 22–0031, ZHKUCC 22–0032, ZHKUCC 22–0033, ZHKUCC 22–0034, ZHKUCC 22–0036 and ZHKUCC 22–0037.

Notes – The eleven isolates obtained in this study developed an independent clade in *Pestalotiopsis* phylogenetic tree with low statistical support (Fig 3). *Pestalotiopsis sabal* is phylogenetically separated from *P. thailandica* and *P. rhizophorae* (Fig 3). Further confirmation with PHI analysis showed that there is no evidence of significant genetic recombination (Fw =0.616) between our species and its closely related species. The number of apical appendages of *P. sabal* is 1–3, while the number of sister clade *P. thailandica* is 1–2, and the size of basal cells is also different (Table 3). Combining both phylogenic evidence and morphology *P. sabal* was identified as a new species.

Pathogenicity test

All six tested *Neopestalotiopsis* and *Pestalotiopsis* species were weakly pathogenic on *Sabal mexicana* leaves. One month after inoculation with the spore suspension, no lesions appeared on the plants (Fig. 11). Ten days after inoculation with mycelium plugs, the wounded leaflets developed small lesions at the pinholes. After 15 days of inoculation, the wounded segments developed irregular brown lesions with black lesions. After 20 days of inoculation, the lesions on wounded inoculated segments were expanded. The area of the brown lesions turned black, and local necrosis appeared. From 25 to 30 days after inoculation, the lesions on the inoculated wounded segments continued to expand, but the scope was still small, necrosis was aggravated. Symptoms on inoculated plants were similar to those observed on the naturally infected leaves of *S. mexicana*. All none-wounded segments did not show lesions after infection. Similarly, all control leaflets remained asymptomatic. Fungal colonies were reisolated from all symptomatic leaves and were found to be morphologically identical to the original isolates inoculated, thus fulfilling the requirements of Koch's postulates.

Discussion

In the present study, *Neopestalotiopsis* and *Pestalotiopsis* species were isolated from *Arecaceae* hosts as saprobes and pathogens. Species delineations were based on multigene phylogeny of ITS, *tub2* and *tef* 1-α sequence data, morphology, and recombination analysis (Maharachchikumbura et al. 2021, Bhunjun et al. 2022). A total of six *Neopestalotiopsis* isolates and 22 *Pestalotiopsis* isolates were characterized and identified. These isolates were identified as two *Neopestalotiopsis* species and four *Pestalotiopsis* species including two novel species: *P. guangdongensis*, *P. sabal*; three new host records *N. formicidarum, P. diploclisiae, P. kandelicola*, and an undermined *Neopestalotiopsis* species.

Recent studies have mentioned that ITS, *tub2* and *tef* 1-α combined gene sequences can better resolve pestalotioid species (Li et al. 2021). However, we found that phylogenetic analysis of these three gene combinations, resulted in poor resolution of some species in *Neopestalotiopsis* and *Pestalotiopsis*. Therefore, additional genes may be needed for better definition (Liu et al. 2017, Norphanphoun et al. 2019, Belisário et al. 2020, Gerardo-Lugo et al. 2020, Huanaluek et al. 2021, Manawasinghe et al. 2021). These three regions alone may not be able to provide a better resolution for species delineation and therefore may have to use polyphasic approach as suggested by Maharachchikumbura et al. (2021) and Bhunjun et al. (2022). Although the overlapping morphological characteristics used to define species have a certain degree of plasticity (Hu et al. 2007), in previous studies under the same growth conditions as previous studies, a thorough morphological characterization is necessary to identify new species (Koukol & Delgado 2021). Several studies have shown that it is necessary to include additional analyses such as recombination to resolve low phylogenetic support (Chethana et al. 2021, Maharachchikumbura et al. 2021, Manawasinghe et al. 2021, Prasannath et al. 2021). Therefore, in this study it is after a careful comparison of the morphology of the species with those of the other sister species, and in combination with the results of phylogenetic analysis and PHI index these three new species were introduced.

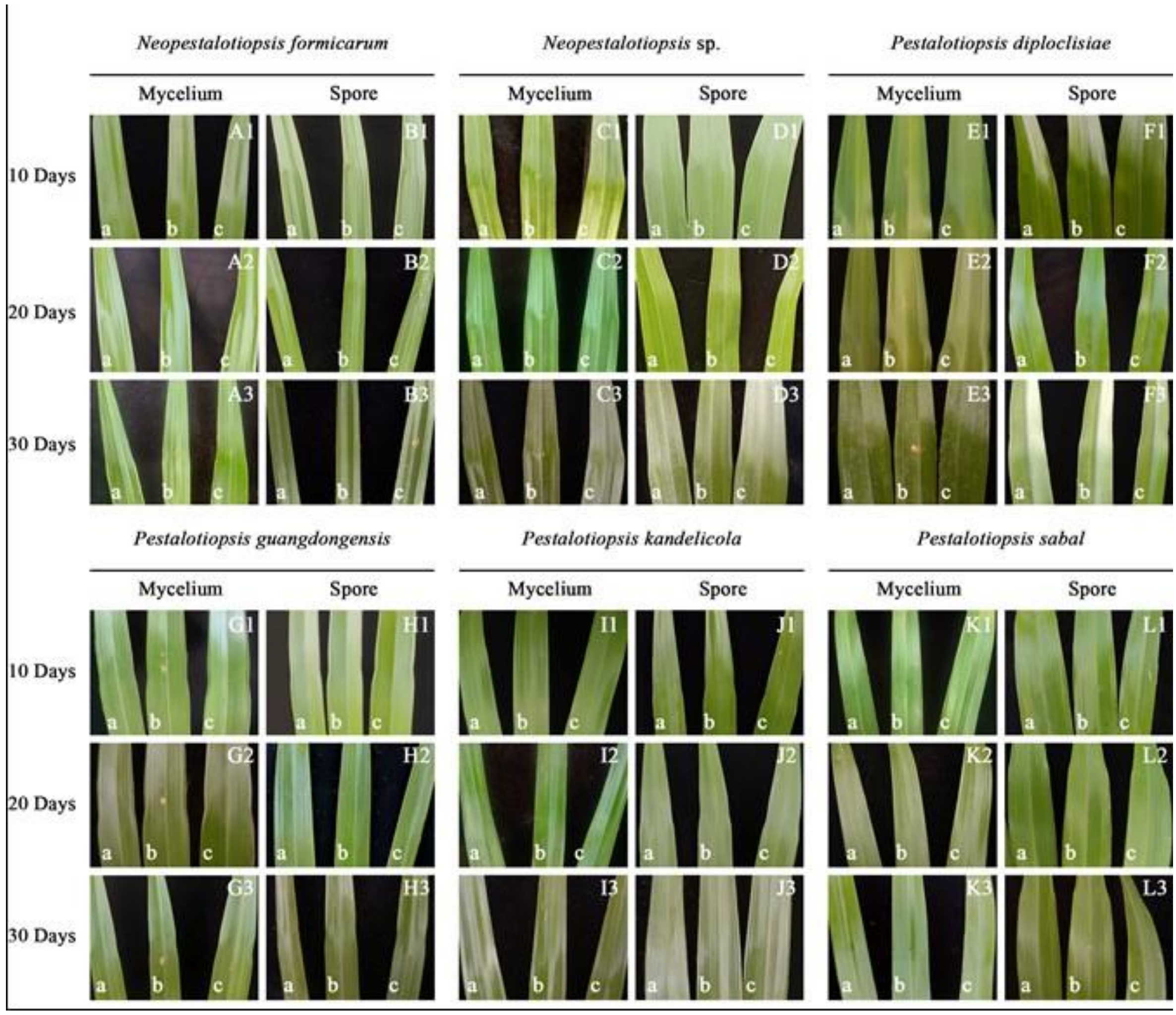

Fig. 11 – Pathogenicity test results of pestalotioid species inoculated on potted *Sabal mexicana* leaves. A1–A3 *Neopestalotiopsis formicidarum* mycelium plugs pathogenicity 10, 20 and 30 days. B1–B3 *N. formicidarum* spore suspension pathogenicity 10, 20 and 30 days. C1–C3 *Neopestalotiopsis* sp. mycelium plugs pathogenicity 10, 20 and 30 days. D1–D3 *Neopestalotiopsis* sp. spore suspension pathogenicity 10, 20 and 30 days. E1–E3 *Pestalotiopsis diploclisiae* mycelium plugs pathogenicity 10, 20 and 30 days. F1–F3 *P. diploclisiae* spore suspension pathogenicity 10, 20 and 30 days. G1–G3 *P. guangdongensis* mycelium plugs pathogenicity 10, 20 and 30 days. H1–H3 *P. guangdongensis* spore suspension pathogenicity 10, 20 and 30 days. I1–I3 *P. kandelicola* mycelium plugs pathogenicity 10, 20 and 30 days. J1–J3 *P. kandelicola* spore suspension pathogenicity 10, 20 and 30 days. K1–K3 *P. sabal* mycelium plugs pathogenicity 10, 20 and 30 days. L1–L3 *P. sabal* spore suspension pathogenicity 10, 20 and 30 days. (a) Non-wounded. (b) Wounded. (c) Control.

Neopestalotiopsis was introduced by Maharachchikumbura et al. (2014) based on morphology and multi-site phylogenetic analysis. Simultaneously *Pestalotiopsis* was divided into three genera, namely *Pestalotiopsis*, *Neopestalotiopsis*, and *Pseudopestalotiopsis*. Over the last few years, species identification and characterization of *Neopestalotiopsis* and *Pestalotiopsis* were based on the phylogenetic analysis of the combined ITS, *tub2* and *tef* 1-α, which resulted in the introduction of many species into these genera (Li et al. 2021, Prasannath et al. 2021). Therefore, to avoid confusions and conflicts in the taxonomy of this genus, we introduced the low-resolution clade as *Neopestalotiopsis* sp. following Gerardo-Lugo et al. (2020). However, it is necessary to develop species delineation approaches to this genus as they are commonly isolated pathogens from many economically important crops.

Jayawardena et al. (2016) reported that *Neopestalotiopsis vitis* causes leaf spots on *Vitis vinifera* in China. In France, various *Neopestalotiopsis* species related to grape stem disease have also been isolated (Maharachchikumbura et al. 2016). Akinsanmi et al. (2017) discovered *N. macadamiae* and *Pestalotiopsis macadamiae* that cause *Macadamia* blight in Australia. Solarte et al. (2018) showed that Colombian Guava scab is caused by several *Pestalotiopsis* and *Neopestalotiopsis* species. *Neopestalotiopsis rosicola* has been reported to causing rose stem canker in China (Jiang et al. 2018). Chen et al. (2018) reported that *N. clavispora* and other pestalotioid species cause gray blight on *Chinese camellia*. Belisario et al. (2020) prove that *N. rosae* and *N. protearum*, and other unidentified species can infect uninjured leaves of eucalyptus under long-term leaf wetting. In addition, this study also tested the pathogenicity of six species from different hosts and found that all tested species caused similar symptoms. Santos et al. (2020) have also been determined that these species can infect *Rose*, *Nepenthes australia* and *Eucalyptus* in older cuttings under conditions that are not conducive to infection. In Portugal, recently reported a new *Pestalotiopsis* species, *P. pini*, was recently reported, which causes stem blight and trunk necrosis of pine trees (Silva et al. 2020). In addition, a common disease in Brazilian nurseries has been attributed to an unidentified *Pestalotiopsis* and is considered a secondary and opportunistic pathogen (Alfenas et al. 2009, Santos et al. 2020). These data revealed that pestalotioid taxa are important as woody host pathogens worldwide.

The present study obtained diseased leaf samples from *Sabal mexicana* plants. Pathogenicity assays confirmed that all the inoculated isolates had shown weak pathogenicity on *Sabal mexicana* leaves when the tissues are wounded and when mycelial plugs were used. They developed brown and black spots and caused local necrosis symptoms similar to those from the collection site. However, the lesion size was smaller than in the field. When using the spore suspension in the pathogenicity tests, there were no signs of infestation on the live *Sabal mexicana* for up to a month. Based on these observations and combined with the study of Santos et al. (2020), we speculate that this could be due to the *Neopestalotiopsis* and *Pestalotiopsis* being opportunistic pathogens. The opportunistic fungal pathogens can live inside the plant as endophytes without causing any damage and when times are favorable for the micro-fungi, they can become pathogenic (Alfenas et al. 2009, Santos et al. 2020). This could be the reason why they did not cause any symptoms on uninjured tissues even with the mycelial plug. It has also been postulated that fungi may migrate through the vascular system of plants and cause lesions at points further from the inoculation point (Santos et al. 2020) to act as a latent pathogen in which symptoms are developed after a certain period from inoculation. Therefore, more in-depth research is required to understand the pathogenic mechanism of *Neopestalotiopsis* and *Pestalotiopsis*. In addition, more attention and research should be aimed at morphological characteristics, such as the spore size and ratio, and the number and length of appendages, needs more research. Therefore, further studies are necessary to understand how to resolve the taxonomic position of each species in phylogenetic analysis and how to make better use of morphological features that are the keys to identifying species within these genera.

Acknowledgements

This work was funded by the High-level Talents in Zhongkai University of Agriculture and Engineering (Grant no. J2201080102). I.S. Manawasinghe would like to thank the Research Project of the Innovative Institute for Plant Health (KA21031H101) and the project of the Zhongkai University of Agriculture and Engineering, Guangzhou, China (KA210319288).

References

Akinsanmi OA, Nisa S, Jeff-Ego OS, Shivas RG, Drenth A. 2017 – Dry flower disease of *Macadamia* in Australia caused by *Neopestalotiopsis macadamiae* sp. nov. and *Pestalotiopsis macadamiae* sp. nov. Plant Dis 101(1), 45–53.

Alfenas A, Zauza E, Mafia R, Assis T. 2009 – *Clonagem e doenças do eucalipto*. UFV, Brazil: Viçosa.
Amrutha P, Vijayaraghavan R. 2018 – Evaluation of Fungicides and Biocontrol Agents against *Neopestalotiopsis clavispora* Causing Leaf Blight of Strawberry *Fragaria x ananassa* Duch. – Int. J. Curr. Microbiol. App. Sci 7(08), 622–628. Doi 10.20546/ijcmas.2018.708.067
Ariyawansa HA, Hyde, KD, Jayasiri SC, Buyck B et al. 2015 – Fungal diversity notes 111–252 – taxonomic and phylogenetic contributions to fungal taxa. Fungal Divers 75(1), 27–274. Doi 10.1007/s13225-015-0346-5
Ariyawansa HA, Hyde KD. 2018 – Additions to *Pestalotiopsis* in Taiwan. Mycosphere 9(5), 999–1013. Doi 10.5943/mycosphere/9/5/4
Ayoubi N, Soleimani MJ. 2016 – Strawberry fruit rot caused by *Neopestalotiopsis iranensis* sp. nov., and *N. mesopotamica*. Curr Microbiol 72(3), 329–336.
Bacon CD, Bailey CD. 2006 – Taxonomy and conservation: A case study from *Chamaedorea alternans*. Ann Bot-London 98(4), 755–763. Doi 10.1093/aob/mcl158
Baker WJ, Dransfield J. 2016 – Beyond *Genera Palmarum*: progress and prospects in palm systematics. Bot J Linn Soc 182(2), 207–233. Doi 10.1111/boj.12401
Basavand E, Pakdin-Parizi A, Mirhosseini HA, Dehghan-Niri M. 2020 – Occurrence of leaf spot disease on date palm caused by *Neopestalotiopsis clavispora* in Iran. J Phytopathol 102(3), 959–959. Doi 10.1007/s42161-020-00530-5
Basu S, Sengupta R, Zandi P. 2014 – "*Arecaceae*: The majestic family of palms".
Belisário R, Aucique-Pérez CE, Abreu LM, Salcedo SS et al. 2020 – Infection by *Neopestalotiopsis* spp. occurs on unwounded eucalyptus leaves and is favoured by long periods of leaf wetness. Plant Pathol 69(2), 194–204. Doi 10.1111/ppa.13132
Bezerra JDP, Machado AR, Firmino AL, Rosado AWC et al. 2018 – Mycological Diversity Description I. Acta Bot Bras 32(4), 656–666. Doi 10.1590/0102-33062018abb0154
Bhunjun CS, Niskanen T, Suwannarach N, Wannathes N et al. 2022 – The numbers of fungi: are the most speciose genera truly diverse? Fungal Divers 1–76.
Carbone I, Kohn L. 1999 – A method for designing primer sets for speciation studies in filamentous ascomycetes. Mycologia 91, 553–556. Doi 10.1080/00275514.1999.12061051
Chaiwan N, Wanasinghe DN, Mapook A, Jayawardena RS et al. 2020 – Novel species of *Pestalotiopsis* fungi on *Dracaena* from Thailand. Mycology 11(4), 306–315. Doi 10.1080/21501203.2020.1801873
Chen YJ, Zeng L, Shu N, Jiang My et al. 2018 – *Pestalotiopsis*-like species causing gray blight disease on *Camellia sinensis* in China. Plant Dis 102(1), 98–106.
Chen YY, Maharachchikumbura SSN, Liu JK, Hyde KD et al. 2017 – Fungi from Asian Karst formations I. *Pestalotiopsis photinicola* sp. nov., causing leaf spots of *Photinia serrulata*. Mycosphere 8, 103–110. Doi 10.5943/mycosphere/8/1/9
Chethana KWT, Manawasinghe IS, Hurdeal VG, Bhunjun CS et al. 2021 – What are fungal species and how to delineate them? Fungal Divers 109(1), 1–25. Doi 10.1007/s13225-021-00483-9
Choi YW, Hyde KD, Ho WWH. 1999 – Single spore isolation of fungi. *Fungal Divers* 3, 29–38.
Crous PW, Wingfield MJ, Le Roux JJ, Richardson DM et al. 2015 – Fungal Planet description sheets: 371–399. Persoonia 35(1), 264–327.
Crous PW, Wingfield MJ, Chooi YH, Gilchrist CLM et al. 2020 – Fungal Planet description sheets: 1042–1111. Persoonia 44, 301–459. Doi 10.3767/persoonia.2020.44.11
Darapanit A, Boonyuen N, Leesutthiphonchai W, Nuankaew S, Piasai O. 2021 – Identification, pathogenicity and effects of plant extracts on *Neopestalotiopsis* and *Pseudopestalotiopsis* causing fruit diseases. Sci Rep-UK 11(1), 22606. Doi 10.1038/s41598-021-02113-5
Das K, Lee SY, Jung HY. 2020 – *Pestalotiopsis kaki* sp. nov., a Novel Species Isolated from Persimmon Tree *Diospyros kaki*) Bark in Korea. Mycobiology 49(1), 54–60. Doi 10.1080/12298093.2020.1852703
De Silva NI, Maharachchikumbura SSN, Thambugala KM, Bhat DJ et al. 2021 – Morphomolecular taxonomic studies reveal a high number of endophytic fungi from *Magnolia candolli* and

M. garrettii in China and Thailand. Mycosphere 12(1), 163–237. Doi 10.5943/mycosphere/12/1/3
Dransfield J, Uhl NW, Asmussen CB, Baker WJ et al. 2008 – *Genera Palmarum-The Evolution and Classification of the Palms.* London, UK: Royal Botanic Gardens, Kew.
Eriksson O, Hawksworth DL. 1986 – An alphabetical list of the generic names of ascomycetes. 5, 3–111.
Freitas EFS, Da Silva M, Barros MVP, Kasuya MCM. 2019 – *Neopestalotiopsis hadrolaeliae* sp. nov., a new endophytic species from the roots of the endangered orchid *Hadrolaelia jongheana* in Brazil. Phytotaxa 416(3), 211–220. Doi 10.11646/phytotaxa.416.3.2
Fröhlich J, Hyde KD. 2000 – *Palm microfungi.* The University of Hong Kong: Fungal Diversity Press.
Geng K, Zhang B, Song Y, Hyde KD et al. 2013 – A new species of *Pestalotiopsis* from leaf spots of *Licuala grandis* from Hainan, China. Phytotaxa 88(3), 49–54.
Gerardo-Lugo SS, Tovar-Pedraza JM, Maharachchikumbura SSN, Apodaca-Sánchez MA et al. 2020 – Characterization of *Neopestalotiopsis* species associated with mango grey leaf spot disease in Sinaloa, Mexico. Pathogens 9(10), 788. Doi 10.3390/pathogens9100788
Glass NL, Donaldson GC. 1995 – Development of primer sets designed for use with the PCR to amplify conserved genes from filamentous ascomycetes. Appl Environ Microb 61(4), 1323–1330.
Griffiths DA, Swart HJ. 1974a – Conidial structure in two species of *Pestalotiopsis*. T Brit Mycol Soc 62(2), 295–IN220.
Griffiths DA, Swart HJ. 1974b – Conidial structure in Pestalotia pezizoides. T Brit Mycol Soc 63. Doi 10.1016/S0007-1536(74)80149-X
Gualberto GF, Catarino ADEM, Sousa TF, Cruz JC et al. 2021 – *Pseudopestalotiopsis gilvanii* sp. nov. and *Neopestalotiopsis formicarum* leaves spot pathogens from guarana plant: a new threat to global tropical hosts. Phytotaxa 489(2), 121–139. Doi 10.11646/phytotaxa.489.2.2
Guba EF. 1960 – Monograph of Monochaetia and Pestalotia. Mycologia 52, 966. Doi 10.2307/3755860
Guo JW, Yang LF, Liu YH, Yang J et al. 2016 – First report of pseudostem black spot caused by *Pestalotiopsis microspora* on Tsao-ko in Yunnan, China. Plant Dis 100(5), 1021–1021.
Gutiérrez del Pozo D, Martín-Gómez J, Tocino Á, Cervantes E. 2020 – Seed Geometry in the *Arecaceae*. Horticulturae 6(4), 64. Doi 10.3390/horticulturae6040064
Haq IU, Ijaz S. 2020 – Etiology and Integrated Management of Economically Important Fungal Diseases of Ornamental Palms. Springer.
Harishchandra DL, Aluthmuhandiram JVS, Yan J, Hyde KD. 2020 – Molecular and morpho-cultural characterisation of *Neopestalotiopsis* and *Pestalotiopsis* species associated with ornamental and forest plants in China.
Hassan NSM, Hossain MS, Balakrishnan V, Zuknik MH et al. 2021 – Influence of Fresh Palm Fruit Sterilization in the Production of Carotenoid-Rich Virgin Palm Oil. Foods 10(11), 2838. Doi 10.3390/foods10112838
Hu H, Jeewon R, Zhou D, Zhou T, Hyde KD. 2007 – Phylogenetic diversity of endophytic *Pestalotiopsis* species in *Pinus armandii* and *Ribes* spp.: evidence from rDNA and β-tubulin gene phylogenies. Fungal Divers 24, 1–22.
Huanaluek N, Jayawardena RS, Maharachchikumbura SSN, Harishchandra D. 2021 – Additions to pestalotioid fungi in Thailand: *Neopestalotiopsis hydeana* sp. nov. and *Pestalotiopsis hydei* sp. nov. Phytotaxa 479, 23–43. Doi 10.11646/phytotaxa.479.1.2
Huelsenbeck JP, Ronquist F. 2001 – MRBAYES: Bayesian inference of phylogenetic trees. Bioinformatics 17(8), 754–755.
Huson DH, Bryant D. 2006 – Application of phylogenetic networks in evolutionary studies. Mol Biol Evol 23(2), 254–267.
Hyde KD, Taylor JE, Fröhlich J. 2000 – Genera of ascomycetes from palm. The University of Hong Kong: Fungal Diversity Press.

Hyde KD, Hongsanan S, Jeewon R, Bhat DJ et al. 2016 – Fungal diversity notes 367–490: taxonomic and phylogenetic contributions to fungal taxa. Fungal Divers 80(1), 1–270. Doi 10.1007/s13225-016-0373-x

Hyde KD, Norphanphoun C, Maharachchikumbura SSN, Bhat DJ et al. 2020a – Refined families of Sordariomycetes. Mycosphere 11(1), 305–1059. Doi 10.5943/mycosphere/11/1/7

Hyde KD, Jeewon R, Chen YJ, Bhunjun CS et al. 2020b – The numbers of fungi: is the descriptive curve flattening? Fungal Divers 103(1), 219–271. Doi 10.1007/s13225-020-00458-2

Ismail SI, Zulperi D, Norddin S, Ahmad-Hamdani S. 2017 – First report of *Neopestalotiopsis saprophytica* causing leaf spot of Oil Palm *Elaeis guineensis*) in Malaysia. Plant Dis 101(10), 1821–1822. Doi 10.1094/pdis-02-17-0271-pdn

Jaklitsch WM, Gardiennet A, Voglmayr H. 2016 – Resolution of morphology-based taxonomic delusions: *Acrocordiella*, *Basiseptospora*, *Blogiascospora*, *Clypeosphaeria*, *Hymenopleella*, *Lepteutypa*, *Pseudapiospora*, *Requienella*, *Seiridium* and *Strickeria*. Persoonia 37(1), 82–105.

Jayasiri SC, Hyde KD, Ariyawansa HA, Bhat J et al. 2015 – The Faces of Fungi database: fungal names linked with morphology, phylogeny and human impacts. Fungal Divers 74(1), 3–18.

Jayawardena RS, Liu M, Maharachchikumbura SSN, Zhang W et al. 2016 – *Neopestalotiopsis vitis* sp. nov. causing grapevine leaf spot in China. Phytotaxa 258(1), 63–74.

Jayawardena RS, Hyde KD, de Farias ARG, Bhunjun CS et al. 2021 – What is a species in fungal plant pathogens? Fungal Divers 109(1), 239–266. Doi 10.1007/s13225-021-00484-8

Jiang N, Bonthond G, Fan XL, Tian CM. 2018 – *Neopestalotiopsis rosicola* sp. nov. causing stem canker of *Rosa chinensis* in China. Mycotaxon 133(2), 271–283.

Jiang N, Fan X, Tian C. 2021 – Identification and Characterization of Leaf-Inhabiting Fungi from *Castanea* Plantations in China. J. Fungi 7(1), 64. Doi 10.3390/jof7010064

Koukol O, Delgado G. 2021 – Why morphology matters: the negative consequences of hasty descriptions of putative novelties in asexual ascomycetes. IMA Fungus 12(1), 26. Doi 10.1186/s43008-021-00073-z

Kumar V, Cheewangkoon R, Gentekaki E, Maharachchikumbura SSN et al. 2019 – *Neopestalotiopsis alpapicalis* sp. nov. a new endophyte from tropical mangrove trees in Krabi Province Thailand – Phytotaxa 393(3), 251–262. Doi 10.11646/phytotaxa.393.3.2

Li L, Pan H, Chen MY, Zhong CH. 2016 – First report of *Pestalotiopsis microspora* causing postharvest rot of kiwifruit in Hubei Province, China. Plant Dis 100(10), 2161.

Li L, Yang Q, Li H. 2021 – Morphology, Phylogeny, and Pathogenicity of Pestalotioid Species on *Camellia oleifera* in China. J. Fungi 7(12), 1080. Doi 10.3390/jof7121080

Liu F, Hou L, Raza M, Cai L. 2017 – *Pestalotiopsis* and allied genera from *Camellia*, with description of 11 new species from China. Sci Rep-UK 7(1), 866. Doi 10.1038/s41598-017-00972-5.

Liu F, Bonthond G, Groenewald JZ, Cai L, Crous PW. 2019 – *Sporocadaceae*, a family of coelomycetous fungi with appendage-bearing conidia. Stud Mycol 92, 287–415. Doi 10.1016/j.simyco.2018.11.001

Liu JK, Hyde KD, Jones EB, Ariyawansa HA et al. 2015 – Fungal diversity notes 1–110: taxonomic and phylogenetic contributions to fungal species. Fungal Divers 72(1), 1–197.

Liu X, Tibpromma S, Zhang F, Xu J et al. 2021 – *Neopestalotiopsis cavernicola* sp. nov. from Gem Cave in Yunnan Province, China. Phytotaxa 512(1), 1–27.

Lu LM, Chen GQ, Hu XR, Du DC et al. 2015 – Identification of *Pestalotiopsis clavispora* causing brown leaf spot on Chinese bayberry in China. Can J Plant Pathol 37(3), 397–402.

Ma XY, Maharachchikumbura SSN, Chen BW, Hyde KD et al. 2019 – Endophytic pestalotiod taxa in *Dendrobium* orchids. Phytotaxa 419(3), 268–286.

Maharachchikumbura SSN, Guo LD, Cai L, Chukeatirote E et al. 2012 – A multi-locus backbone tree for *Pestalotiopsis*, with a polyphasic characterization of 14 new species. Fungal Divers 56(1), 95–129. Doi 10.1007/s13225-012-0198-1

Maharachchikumbura SSN, Chukeatirote E, Guo LD, Crous PW et al. 2013a – *Pestalotiopsis* species associated with *Camellia sinensis* tea – Mycotaxon 123(1), 47–61.

Maharachchikumbura SSN, Guo LD, Chukeatirote E, McKenzie EHC, Hyde KD. 2013b – A destructive new disease of *Syzygium samarangense* in Thailand caused by the new species *Pestalotiopsis samarangensis*. Trop Plant Pathol 38(3), 227–235. Doi 10.1590/s1982-56762013005000002

Maharachchikumbura SSN, Guo LD, Chukeatirote E, Hyde KD. 2013c – Improving the backbone tree for the genus *Pestalotiopsis*; addition of *P. steyaertii* and *P. magna* sp. nov. Mycol Prog 13(3), 617–624. Doi 10.1007/s11557-013-0944-0

Maharachchikumbura SSN, Zhang YM, Wang Y, Hyde KD. 2013d – *Pestalotiopsis anacardiacearum* sp. nov. *Amphisphaeriaceae*) has an intricate relationship with *Penicillaria jocosatrix*, the mango tip borer. Phytotaxa 99(2), 49–57. Doi 10.11646/phytotaxa.99.2.1

Maharachchikumbura SSN, Hyde KD, Groenewald JZ, Xu J, Crous PW. 2014 – *Pestalotiopsis* revisited. Stud Mycol 79, 121–186. Doi 10.1016/j.simyco.2014.09.005

Maharachchikumbura SSN, Larignon P, Hyde KD, Al-Sadi AM, Liu ZY. 2016 – Characterization of *Neopestalotiopsis*, *Pestalotiopsis* and *Truncatella* species associated with grapevine trunk diseases in France. Phytopathol Mediterr 55(3), 380–390.

Maharachchikumbura SSN, Chen Y, Ariyawansa HA, Hyde KD et al. 2021 – Integrative approaches for species delimitation in Ascomycota. Fungal Divers 109(1), 155–179. Doi 10.1007/s13225-021-00486-6

Manawasinghe IS, Jayawardena RS, Li HL, Zhou YY et al. 2021 – Microfungi associated with *Camellia sinensis*: A case study of leaf and shoot necrosis on Tea in Fujian, China. Mycosphere 12(1), 430–518. Doi 10.5943/mycosphere/12/1/6

Mendes J, Portilho A, Aguiar-Dias A, Sampaio K, Farias L. 2019 – *Arecaceae*: Uma EstratÉgia Diferenciada Para O Ensino De BotÂnica Em Uma Escola De Ensino MÉdio Na Ilha De Cotijuba, ParÁ, Brasil. Enciclopédia Biosfera 16(29), 2226–2240. Doi 10.18677/EnciBio_2019A170

Miller MA, Pfeiffer W, Schwartz T. 2010 – Creating the CIPRES Science Gateway for inference of large phylogenetic trees. In Proceedings of the 2010 gateway computing environments workshop (GCE), pp. 1c8.

Mycobank. 2022 – [Online]. Available: https://www.mycobank.org/ (Accessed on July 20, 2022).

Nadot S, Alapetite E, Baker WJ, Tregear JW, Barfod AS. 2016 – The palm family *Arecaceae*): a microcosm of sexual system evolution. Bot J Linn Soc 182(2), 376–388. Doi 10.1111/boj.12440

Nag Raj TR. 1985 – Redisposals and redescriptions in the Monochaetia-Seiridium, Pestalotia-Pestalotiopsis complexes. II. *Pestalotiopsis besseyii* Guba) comb. nov. and *Pestalosphaeria varia* sp. nov. Mycotaxon 22, 52–63.

Norphanphoun C, Jayawardena RS, Chen Y, Wen TC et al. 2019 – Morphological and phylogenetic characterization of novel pestalotioid species associated with mangroves in Thailand. Mycosphere 10(1), 531–578. Doi 10.5943/mycosphere/10/1/9

Pandian RTP, Thube SH, Bhavishya, Merinbabu et al. 2021 – First report of *Phytophthora palmivora* (E. J. Butler) E. J. Butler, 1919 causing fruit rot in *Areca triandra* Roxb. ex Buch.-Ham. from India. Australas Plant Path 50(4), 495–499. Doi 10.1007/s13313-021-00802-3

Pornsuriya C, Chairin T, Thaochan N, Sunpapao A. 2020 – Identification and characterization of *Neopestalotiopsis* fungi associated with a novel leaf fall disease of rubber trees *Hevea brasiliensis*) in Thailand. J Phytopathol 168(7-8), 416–427.

Prasannath K, Shivas RG, Galea VJ, Akinsanmi OA. 2021 – *Neopestalotiopsis* species sssociated with flower diseases of *Macadamia integrifolia* in Australia. J. Fungi 7(9), 771. Doi 10.3390/jof7090771

Quaedvlieg W, Binder M, Groenewald JZ, Summerell BA et al. 2014 – Introducing the consolidated species concept to resolve species in the *Teratosphaeriaceae*. Persoonia 33(1), 1–40.

Rajesh MK, Ramesh SV, Perera L, Kole C. 2021 – The Coconut Genome. Springer.

Ran SF, Maharachchikumbura SSN, Ren YL, Liu H et al. 2017 – Two new records in *Pestalotiopsidaceae* associated with *Orchidaceae* disease in Guangxi Province, China. Mycosphere 8(1), 121–130. Doi 10.5943/mycosphere/8/1/11

Rayner RW. 1970 – A mycological colour chart. Kew, UK Commonwealth Mycological Institute & British Mycological Society.

Reddy MS, Murali TS, Suryanarayanan TS, Govinda Rajulu MB, Thirunavukkarasu N. 2016 – *Pestalotiopsis* species occur as generalist endophytes in trees of Western Ghats forests of southern India. Fungal Ecol 24, 70–75. Doi 10.1016/j.funeco.2016.09.002

Santos GS, Mafia RG, Aguiar AM, Zarpelon TG et al. 2020 – Stem rot of eucalyptus cuttings caused by *Neopestalotiopsis* spp. in Brazil. J Phytopathol 168(6), 311–321.

Selmaoui K, Touati J, Chliyeh M, TouhamiI A et al. 2014 – Study of *Pestalotiopsis palmarum* pathogenicity on *Washingtonia robusta* Mexican palm – Int J Pure Appl Biosci 2, 138–145.

Senanayake IC, Lian TT, Mai XM, Jeewon R et al. 2020 – New geographical records of *Neopestalotiopsis* and *Pestalotiopsis* species in Guangdong Province, China. Asian J. Mycol 3(1), 512–533. Doi 10.5943/ajom/3/1/19

Shu J, Yu Z, Sun W, Zhao J et al. 2020 – Identification and characterization of pestalotioid fungi causing leaf spots on mango in southern China. Plant Dis 104(4), 1207–1213.

Silva AC, Diogo E, Henriques J, Ramos AP et al. 2020 – *Pestalotiopsis pini* sp. nov., an Emerging Pathogen on Stone Pine *Pinus pinea* L. Forests 11(8), 805. Doi 10.3390/f11080805

Silvério ML, Calvacanti MAdQ, Silva GAd, Oliveira RJVd, Bezerra JL. 2016 – A new epifoliar species of *Neopestalotiopsis* from Brazil. Agrotrópica 28(2), 151–158.

Solarte F, Muñoz CG, Maharachchikumbura SSN, Alvarez E. 2018 – Diversity of *Neopestalotiopsis* and *Pestalotiopsis* spp., causal agents of guava scab in Colombia. Plant Dis 102(1), 49–59.

Song Y, Geng K, Hyde KD, Zhao WS et al. 2013 – Two new species of *Pestalotiopsis* from Southern China. Phytotaxa 126(1), 22–30.

Song Y, Maharachchikumbura SSN, Jiang YL, Hyde KD, Wang Y. 2014a – *Pestalotiopsis keteleeria* sp. nov., isolated from *Keteleeria pubescens* in China. Chiang Mai J Sci 41(4), 885–893.

Song Y, Tangthirasunun N, Maharachchikumbura SSN, Jiang YL et al. 2014b – Novel *Pestalotiopsis* species from Thailand point to the rich undiscovered diversity of this chemically creative genus. Cryptogamie Mycol 35(2), 139–149.

Species Fungorum. 2022 – [Online]. Available: http://www.speciesfungorum.org/ (Accessed July 20, 2022).

Stamatakis A, Hoover J, Rougemint J. 2008 – A rapid Bootstrap algorithm for the RAxML Web Servers. *Syst Biol* 75, 558–771.

Stamatakis A. 2014 – RAxML version 8: a tool for phylogenetic analysis and post-analysis of large phylogenies. Bioinformatics 30(9), 1312–1313. Doi 10.1093/bioinformatics/btu033

Steyaert RL. 1949 – Contribution a l'etude monographique de Pestalotia de Not. et Monochaetia Sacc. Truncatella gen. nov. et *Pestalotiopsis* gen. nov. Bulletin du Jardin botanique de l'État a Bruxelles 19(3), 285–347. Doi 10.2307/3666710

Steyaert RL. 1963 – Complementary informations concerning *Pestalotiopsis guepini* Desmazieres) Steyaert and designation of its lectotype. Bulletin du Jardin botanique de l'État a Bruxelles 33(3), 369–373.

Sutton BC. 1980 – The coelomycetes: fungi imperfecti with pycnidia aceruli and stromata. Commonwealth, Survey.

Suwannarach N, Kumla J, Bussaban B, Lumyong S. 2012 – New report of leaf blight disease on eucalyptus *Eucalyptus camaldulensis*) caused by *Pestalotiopsis virgatula* in Thailand. Can J Plant Pathol 34(2), 306–309. Doi 10.1080/07060661.2012.680501

Swofford DL. 2002 – PAUP*. Phylogenetic Analysis Using Parsimony *and Other Methods – Version 4.0b10.

Tibpromma S, Hyde KD, McKenzie EHC, Bhat DJ et al. 2018 – Fungal diversity notes 840–928: micro-fungi associated with *Pandanaceae*. Fungal Divers 93(1), 1–160. Doi 10.1007/s13225-018-0408-6

Tibpromma S, Mortimer PE, Karunarathna SC, Zhan FD et al. 2019 – Morphology and multi-gene phylogeny reveal *Pestalotiopsis pinicola* sp. nov. and a new host record of *Cladosporium anthropophilum* from edible pine *Pinus armandii*) seeds in Yunnan province, China. Pathogens 8(4), 285.

Watanabe K, Motohashi K, Ono Y. 2010 – Description of *Pestalotiopsis pallidotheae*: a new species from Japan. Mycoscience 51(3), 182–188.

Watanabe K, Nozawa S, Hsiang T, Callan B. 2018 – The cup fungus *Pestalopezia brunneopruinosa* is *Pestalotiopsis gibbosa* and belongs to Sordariomycetes. Plos one 13(6), e0197025.

White TJ, Bruns T, Lee S, Taylor J. 1990 – Amplification and direct sequencing of fungal ribosomal RNA genes for phylogenetics. PCR protocols: a guide to methods and applications 18(1), 315–322.

Wijayawardene NN, Hyde KD, Al-Ani LKT, Tedersoo L et al. 2020 – Outline of Fungi and fungus-like taxa. Mycosphere 11(1), 1060–1456. Doi 10.5943/mycosphere/11/1/8

Wijayawardene NN, Hyde KD, Dai DQ, Sánchez-García M et al. 2022 – Outline of Fungi and fungus-like taxa–2021. Mycosphere 13(1), 53–453.

Yang Q, Zeng XY, Yuan J, Zhang Q et al. 2021 – Two new species of *Neopestalotiopsis* from southern China. Biodivers Data J 9, e70446. Doi 10.3897/BDJ.9.e70446

Zhang Q, Yang ZF, Cheng W, Wijayawardene NN et al. 2020 – Diseases of *Cymbopogon citratus Poaceae*) in China: *Curvularia nanningensis* sp. nov. MycoKeys 63, 49.

Zhang YM, Maharachchikumbura SSN, Wei JG, McKenzie EHC, Hyde KD. 2012a – *Pestalotiopsis camelliae*, a new species associated with grey blight of *Camellia japonica* in China. Sydowia 64(2), 335–344.

Zhang YM, Maharachchikumbura SS, Mckenzie EH, Hyde KD. 2012b – A novel species of *Pestalotiopsis* causing leaf spots of *Trachycarpus fortunei*. Cryptogamie Mycol 33(3), 311–318.

Zhang YM, Maharachchikumbura SSN, Tian Q, Hyde KD. 2013 – *Pestalotiopsis* species on ornamental plants in Yunnan Province, China. Sydowia 65, 113–128.